Studying the Effects of Polymerization Temperature, Composition, and Initiation Rate on Network Structure Formation by Free Radical PhotoPolymerization of a Low T_g Monoacrylate/Diacrylate System

by

Rafael Levin

S.B., Materials Science and Engineering
Massachusetts Institute of Technology, 1994

Submitted to the Department of Materials Science and Engineering in Partial Fulfillment of the Requirements for the Degree of

Master of Science
in Materials Science and Engineering

at the
Massachusetts Institute of Technology
May 1994

Signature of Author.....
Department of Materials Science and Engineering
May 6, 1994

Certified by .....
Professor Michael F. Rubner
Department of Materials Science and Engineering
Thesis Advisor

Accepted by .....
Carl V. Thompson II
Professor of Electronic Materials
Chair, Departmental Committee on Graduate Students

Studying the Effects of Polymerization Temperature, Composition, and Initiation Rate on Network Structure Formation by Free Radical PhotoPolymerization of a Low T_g Monoacrylate/Diacrylate System

by

Rafael Levin

Submitted to the Department of Materials Science and Engineering
in May 6, 1994 in Partial Fulfillment of the Requirements for the
Degree of Master of Science in Materials Science and Engineering

Abstract

By employing a simple kinetic study in conjunction with equilibrium tensile modulus measurements, the crosslink density formation during a free radical bulk photocopolymerization of a low T_g monoacrylate/diacrylate system was investigated in light of a simple statistical network model and under the assumption of an ideal entropy elastomer. In particular, the effects on the crosslink density of three important processing controlled parameters, namely, polymerization temperature (in the range above T_g of the fully cured network), irradiation intensity, and conversion level (measured by NIR spectroscopy), have been investigated both theoretically and experimentally. The effects of a fourth parameter, formulation, as defined here by the monoacrylate/diacrylate concentration ratio was discussed from a theoretical perspective.

In addition to interesting phenomenological aspects, such as possible mechanisms by which temperature affects the free radical kinetics and network structure development, some findings from this study may have direct important industrial and commercial implications: 1) The crosslink density as a function of conversion was characterized by a strong positive curvature causing the modulus to be extremely sensitive to the conversion level during the polymerization of the final 20% to 30% of the residual reactive groups. 2) The strong temperature dependence of the various kinetic rate constants involved in the free radical polymerization process cause the crosslink density, and thus the modulus, to be sensitive to the polymerization temperature. In this case, for example, it was found that temperature-activated transfer was responsible for reducing the modulus by a factor of 2 as the polymerization temperature increased by 100°C. 3) Considering photoinitiation in a free radical network-forming polymerization, the irradiation intensity effect on the network crosslink density can be quite dramatic. In this study, however, it was shown that an overwhelming transfer reaction did not allow observation of the initiation rate effect at the relatively low irradiation intensities used. 4) In spite of the complexities involved in directly controlling the free radical polymerization kinetics as compared with simply changing the formulation (concentration of crosslinkers), the statistical model suggests motivations for using the former approach when "designing the network structure". In this study, it was shown that for applications in which a specific crosslink density is desirable at a fixed conversion level, a free radical network-forming system having a high degree of polymerization (D_p) and a low crosslinkers-concentration is more robust to fluctuations in both D_p and conversion relative to a low-D_p-high-crosslinker concentration system, giving the same theoretical crosslink density at the same conversion.

On a more general level, the simple experimental and theoretical framework employed in this study, though highly idealized, proved to be useful and implementable for gaining a better understanding of network structure formation as well as potential ways in which to control the desired structure-determined properties. It is believed that implementation of similar semi-quantitative (and obviously more quantitative) analytical methods as used here, can have promising contributions to the industrial optimization process of even more complicated network forming polymerization systems. Suggestions for future work include further investigation of model predictions beyond those studied here, use of more sophisticated network models in conjunction with more sensitive experimental measurements, employment of macroscopic properties other than equilibrium tensile modulus to monitor the underlying network structure, use of a more informative kinetic study, and investigation of additional systems of higher purity and simplicity under a wider range polymerization temperature, composition, and irradiation intensity.

To my parents, *Samuel* and *Gaby*, who through their unsurpassed love, faith and wisdom, have taught me all those things no one else could ever teach me.

To my Brothers *Daniel* and *Ariel*, whose uncompromising support and sacrifices have nourished me thus far.

To my Grandmothers *Bella* and *Charlotte*, whose warmth I shall cherish forever, and to my late Grandfathers, *Emanuel* and *Emil*, who did not get the chance to witness my graduation, but are always with me in spirit.

Finally, to *Sigal*, my home and future.

May God bless them all with everlasting health, strength, and happiness.

Acknowledgments

My sincere gratitude and appreciation to the Department of Materials Science and Engineering at MIT, and to Department 11145 at AT&T Bell Laboratories for giving me the opportunity to experience cutting edge industrial research while working on this project. In particular, I am deeply indebted to Arturo Hale, Ph.D. and Professor Michael Rubner, my thesis advisors at AT&T and MIT, respectively. I owe both for their inexhaustible confidence and trust in my abilities, and for their constructive and supportive advice every step of the way.

To Lee Blyler, Ph.D., my supervisor at AT&T and to Joe Dhosi, my Coop program advisor at MIT, I thank for their generous help and guidance whenever I was in need.

A special thanks to all other collaborators on this project: Alex Harris, Ph.D., Harvey Bair, Ph.D., and Nick Levinos. Fred Schilling and Mark Paczkowski I thank for their important assistance in the chemical analysis.

Last, but not least, I would like to mention all those who, in one way or another, made a contribution to this thesis, and gave me a most enjoyable educational experience over this past year: Shiro Matsuaka, Ph.D, head of department 11145, Marti Green, Ph.D., my AT&T Coop program mentor, Anne Jacoby, Debbie Simoff, Maureen Chen, Lloyd Shepherd, Ph.D, Xina Quan, Ph.D, Ron Larson, Ph.D, Nancy Hines, Ed Johnson, Ph.D, Val Kuck, Bob Decker, Archer Lynden, Ph.D, You-lung Chen, Ph.D, Sundar Venkataraman, Ph.D, Yussuf Ali, Art Hart, Ph.D, and Kym Starcher.

Table of Contents

Section 1: Introduction 15

1.1 General Background 15
1.2 Study Goals 15

Section 2: Theory 18

2.1 Modeling Polymer Network Structure Formation - An Historical Perspective 19
2.2 The Recursive Network Model as the Theoretical Framework 21
2.2.1 General 21
2.2.2 The Model Itself 22
2.3 The Free Radical Kinetics of the Study Model System 24
2.3.1 Initiation 24
2.3.2 Termination 25
2.3.3 Propagation 25
2.3.4 Transfer Reactions 25
2.4 Temperature and Initiation Rate Effects on the Free Radical Step Rates 27
2.4.1 Initiation Rate Effect 27
2.4.2 Temperature Effect 28
2.5 From Linear to Nonlinear Systems - An Intuitive Perspective 31
2.6 Applying the Model as a Predicting Tool 36
2.6.1 Model Predictions of Crosslink Density as a Function of q, e, af, p 37
2.6.2 Incorporating the Temperature and R_i Effects on the Free Radical Kinetics into the Statistical Network Model 48

Section 3: Experimental Procedure 52

3.1 Choosing the Model System 53
3.2 Preparing the Monomer Solution 55
3.3 Characterizing the System 55
3.4 The Scheme for Generating the Data 56
3.4.1 Using Equilibrium Tensile Modulus as a Macroscopic Gauge of the Crosslink Density 56
3.4.2 Using T_g as Macroscopic Gauge of the Crosslink Density 59
3.4.3 Controlling the Photo-polymerization Process 61
3.4.4 Measuring Conversion 62
3.4.5 Equilibrium Tensile Modulus Measurements 62
3.4.6 T_g Measurements 63
3.4.7 Predicting the Modulus and Calculating q, e, and/or af by Fitting Modulus and Conversion Data to Model Predictions 63

Table of Contents (cont'd)

Section 4: Results and Discussion 65

4.1 Characterization Results 65
4.1.1 Monofunctional Monomer 65
4.1.2 Difunctional Oligomer 67
4.1.3 Monofunctional/Difunctional Solution with Photo-initiator in the Uncured and Cured States 67
4.2 Kinetics (and Thermodynamics) of the Free Radical PhotoPolymerization 68
4.2.1 Polymerization Kinetics as a Function of Temperature 70
4.2.2 Kinetics as a Function of Irradiation Intensity 75
4.3 Modulus Results 76
4.3.1 Modulus as a Function of Conversion 76
4.3.2 Modulus as a Function of the Polymerization Temperature 79
4.3.3 Modulus as a function of irradiation intensity 84
4.4 Error Propagation Analysis 85

Section 5: Conclusion and Recommendations for Future Work 88

5.1 Conclusions 88
5.2 Recommendations for Future Work 91

Appendix A: Calculating the Initiation Rate, R_i 95

Appendix B: NIR Difference and Cured Spectra 96

Appendix C: Model Calculation of Crosslink Density 97

List of Figures and Tables

Figure -2-1. A schematic showing the relationships between the different kinetic model parameters and processing parameters which together predict the network structure and some of its respective structure-controlled macroscopic properties. This study focuses on equilibrium tensile modulus (under the ideal entropy elastomer assumption) as the primary crosslink density controlled macroscopic property. For a comprehensive treatment of The effects of crosslinking density on physical properties of polymers, see E.L. Neilsen's work. 18

Figure 2-2. Network A represents an idealized two-dimensional, monofunctional/difunctional, free-radical polymerized network extending to infinity in the vertical dimension only. Network B is the result of cutting four chains from Network A. As a result, Network B has eight less effective links than network A. Though unrealistic according to the recursive model, in this idealized schematic one can perceive Network B as having an average chain length that is half that of A. Networks A' and B' are the respective perfect networks in which each of the difunctional monomers serves as a four functional crosslinker. Keeping in mind that "infinity" is still defined in the vertical dimension only, A' and B' have the identical number of maximum possible crosslinks, 52. Creating B' from B required eight more links than were necessary in creating A' from A. 32

Figure 2-3. Comparison between the unrealistic ideal model prediction and the statistical model prediction (both calculated for arbitrarily chosen e=0 and af=0.189) giving the absolute value of the full conversion reduction in the crosslink density as a function of D_p, relative to D_p=1000. 36

Figure 2-4. Predicted fraction of maximum crosslink density as a function of conversion for different q values. Calculations were made for af=0.15 and e=0.5. 40

Figure 2-5. Comparison between two curves of predicted maximum crosslink density fraction as a function of conversion. The curve marked "0.92" was calculated for q=0.92 and than multiplied by a constant so that its full conversion crosslink density equals that of the curve calculated for q=0.99. For both curves, af=0.15 and e=0.5.41

Figure 2-6. Predicted fraction of maximum crosslink density as a function of conversion for different af values. Calculations were made for q=0.95 and e=0.5. 42

Figure 2-7. Comparison between two curves of predicted maximum crosslink density fraction as a function of conversion. The curves marked "0.12" and "0.25" were calculated for af=0.12 and 0.25, respectively. These curves were than multiplied by a constant so that their full conversion crosslink density equals that of the curve calculated for af=0.3. For all curves q=0.95 and e=0.5. 42

Figure 2-8. Fraction of maximum crosslink density (calculated relative to af=0.3 and for e=0.5) as a function of conversion, predicted for different combinations of q and af values with the constraint of equal crosslink density at full conversion. 44

Figure 2-9. Full conversion crosslink density (arbitrary scale) as a function of D_p (e=0) for a series of different af values as predicted by the statistical model. 46

Figure 2-10. Flow chart showing the expected effect on the crosslink density as a result of changing the initiation rate. 50

List of Figures and Tables (cont'd)

Figure 3-1. The components and their respective concentrations in the formulation used as the study model system for experimentally investigating effects of photo-polymerization temperature, initiation rate, and conversion on network structure formation. 52

Figure 3-2. Experimental setup for polymerization temperature, initiation rate, and conversion controlled photo-polymerization of thin films. 60

Figure 4-1. Characterization results.[41] **A:** Thermogravimetric analysis. **B and C:** T_g measurement by DSC for fully uncured and fully cured system, respectively. 66

Figure 4-2. Logarithmic plots of residual percentage acrylates versus irradiation exposure time (2.5 mW/cm^2) for different polymerization temperatures. Under the assumptions of the free radical photopolymerization mechanism, the plot should be linear with an absolute value slope equal to $K_p(R_i/2K_t)^{1/2}$ 69

Figure 4-3. Arrhenius plot of the absolute slope (x 10^4) of the rate curves vs. the reciprocal of their respective polymerization temperature (in Kelvin). The slope of the fitted linear curve between 30°C and 90°C is expected to equal $(1/2E_t - E_p)/R$, where E_t is the is the dominating termination activation energy in that temperature regime. 72

Figure 4-4. Logarithmic plots of residual percentage acrylates versus irradiation exposure time (2.5 mW/cm^2) for two different irradiation intensities at two different polymerization temperatures. Under the assumptions of the free radical photopolymerization mechanism, the plot should be linear with an absolute value slope equal to $K_p (R_i/2K_t)^{1/2}$. 75

Figure 4-5. Equilibrium tensile modulus as a function of conversion for films polymerized at 60°C and 105°C, respectively. The ▪ and ◆ shapes of data points for the samples polymerized at 60°C represent two different irradiation intensities of 2.5 and 0.25 mW/cm^2, respectively. Films cured at 105°C were irradiated with a 2.5 mW/cm^2 intensity. The continuous curves are the statistical model predictions generated by fitting appropriate *q* values to the data, while using af=0.189, R_i=5.1 x 10^{-6} molar/s, and assuming e=0. 76

Figure 4-6. Maximum ("post full conversion") equilibrium tensile modulus as a function of the polymerization temperature. Numerical values by the data points represent D_p as calculated from the model predicted q for full conversion, af=0.189, and using e=0. 79

Figure 4-7. Natural logarithm of D_p (predicted from modulus results by the statistical model for full conversion, af=0.189, and e=0) vs. the inverse of the polymerization temperature in Kelvin. 83

Table 2-1 38

Table 2-2 44

Table 4-1 70

Section 1: Introduction

1.1 General Background

The ability to manipulate polymer network, structure-controlled properties such as the thermo-mechanical behavior of entropy elastomers above T_g, has long been recognized as a key to achieving desired materials for extensively used industrial and commercial applications of great importance. Often easy to process, this class of materials can be found incorporated in a myriad of products, be it for protective packaging against mechanical and environmental degradation, electrical and thermal insulation, or any other application ranging from optical fiber coatings,[1,2] to biomaterials used in medicine and dentistry.[3,4,5] Specifically, the photo-polymerization of free-radical, network-forming systems has proven to be extremely useful method for processing these materials due to the gained ability to generate high-resolution, photo-defined polymer networks, the structure of which can potentially be tailored to embody the desired network structure-dependent properties.

While today only some high-tech applications demand relatively strictly controlled network structures to achieve the desired material properties, it can be expected that in years to come, the control of polymer network structures will increasingly play a dominant role as a limiting factor of materials' performance in almost any application. Thus, there are motivations for studying network formation and structure of such systems both by experiment and theoretical modeling. Understanding how different parameters control structural development enables us to achieve desired network properties by manipulating these parameters via both formulation of the participating monomers (the building blocks) and via control of the processing conditions.

1.2 Study Goals

This study is aimed at understanding network structure formation of a photopolymerized monoacrylate/diacrylate model system at temperatures above T_g of the fully cured network. Specifically, there is an attempt to establish crosslink density as a function of curing temperature, rate of initiation, degree of conversion, and formulation as defined here in terms of the relative composition of monofunctional and difunctional (crosslinking) components. Macroscopically, equilibrium tensile modulus measurements under the ideal entropy elastomer assumption is used as the primary indicator of the crosslink density and,

thus, network structure. Experimental results are interpreted in light of a recursive network model, which predicts average structural parameters as a function of monomer composition, degree of conversion, and kinetic parameters, which control the free radical photopolymerization mechanism.

It should be pointed out that over the past few years there has been a continuing theoretical development of more and more mathematically sophisticated models and computer simulations in an attempt to predict network structure formation with an ever increasing accuracy, while relaxing some of the basic assumptions underlying the relatively simple model used here. Experimentally, however, very little if any progress has been made in an attempt to reconcile empirical data with even the simplest model predictions. It seems that the gap that has been growing over time between theoretical and experimental efforts in this area has a two-fold explanation:

From the experimental stand-point, even when ignoring problems strictly associated with the implementation of complex theoretical models into aspects of experimental design, most of the formulations and processing conditions currently used in producing commercial applications tend to embody far more complex systems than would be feasible to study under the available theoretical framework of even the most complicated models. In the industrial laboratory, therefore, the optimization process of tailoring network structure to meet product properties specifications has dominantly followed a route of trial-and-error solutions based on a variety of underlying general guiding principles. Moreover, as demand keeps growing for more specialized network properties and higher product quality at increased production rates and lower costs, usually the number of formulation components increases and processing parameters and procedures become more complex. It is conceivable, for reasons further addressed in the next section, that we are still far from being able to employ a unified, comprehensive model powerful enough to fully explain and manipulate the kinetics and structural development of many complex systems of commercial interest and use today.

From a theoretical standpoint, not only are the most sophisticated models insufficient in coping with the complexities of commercially available applications as already mentioned, but it is also the case that even simple models require a significant number of kinetic and other parameters which are not readily available from the existing empirical data. Further more, as models strive to relax more assumptions, they concomitantly tend to require a growing number of these parameters while becoming mathematically and computationally

more challenging, thus making it even harder to asses their true power of directly by experimentation.

As a result of the above trends, there is a sense that theory and experiment diverge from each other while one can still evidence incremental improvements in product applications, quality, and network properties specializations. Nevertheless, there is a strong underlying notion of a promising potential for a quantum-leap-type advancement enabled by gaining complete understanding of network structure development and its manipulation once the theoretical and experimental efforts meet. In light of this realization, the following study is perceived as forming an initial bridge in an attempt to minimize the gap between these two ends. The theoretical model employed here is simple compared to available models, and subsequently its power depends heavily on the applicability of its underlying assumptions. The advantages, however, of using a simple model are clearly appreciated in light of the relatively simple photopolymerized system of choice for the experimental study. While the chosen system formulation is considerably simpler than most currently used commercial formulations, it was designed to meet the assumptions imposed by the model. This construction of model and experiment is aimed at minimizing the number of required independent parameters while maximizing the applicability of the theory to the experimental setup.

Naturally, the applicability of results and conclusions from this study to the more complex systems of commercial interest is somewhat limited by virtue of the simplicity of the experimental system employed. Nevertheless, this study provides some important insights that are generally relevant to most free-radical, network forming polymerizations, and can be of direct applicability to many of the simpler commercial systems. Moreover, the mere demonstration of the potential usefulness found in directly employing a statistical model in conjunction with experiment to study and control network structure formation, is by itself a goal of this project. It is hard to conceive that this goal would be as achievable at this point by employing a more complicated model system to begin with. It is hoped that, in the future, similar experimental schemes will be directly employed to investigate and optimize network structure controlled properties of more complex systems of commercial applications while using more informative experimental methods to get all the required parameters necessary to be used by the more sophisticated theoretical models which will be powerful enough to encompass the full complexity of these systems.

Section 2: Theory

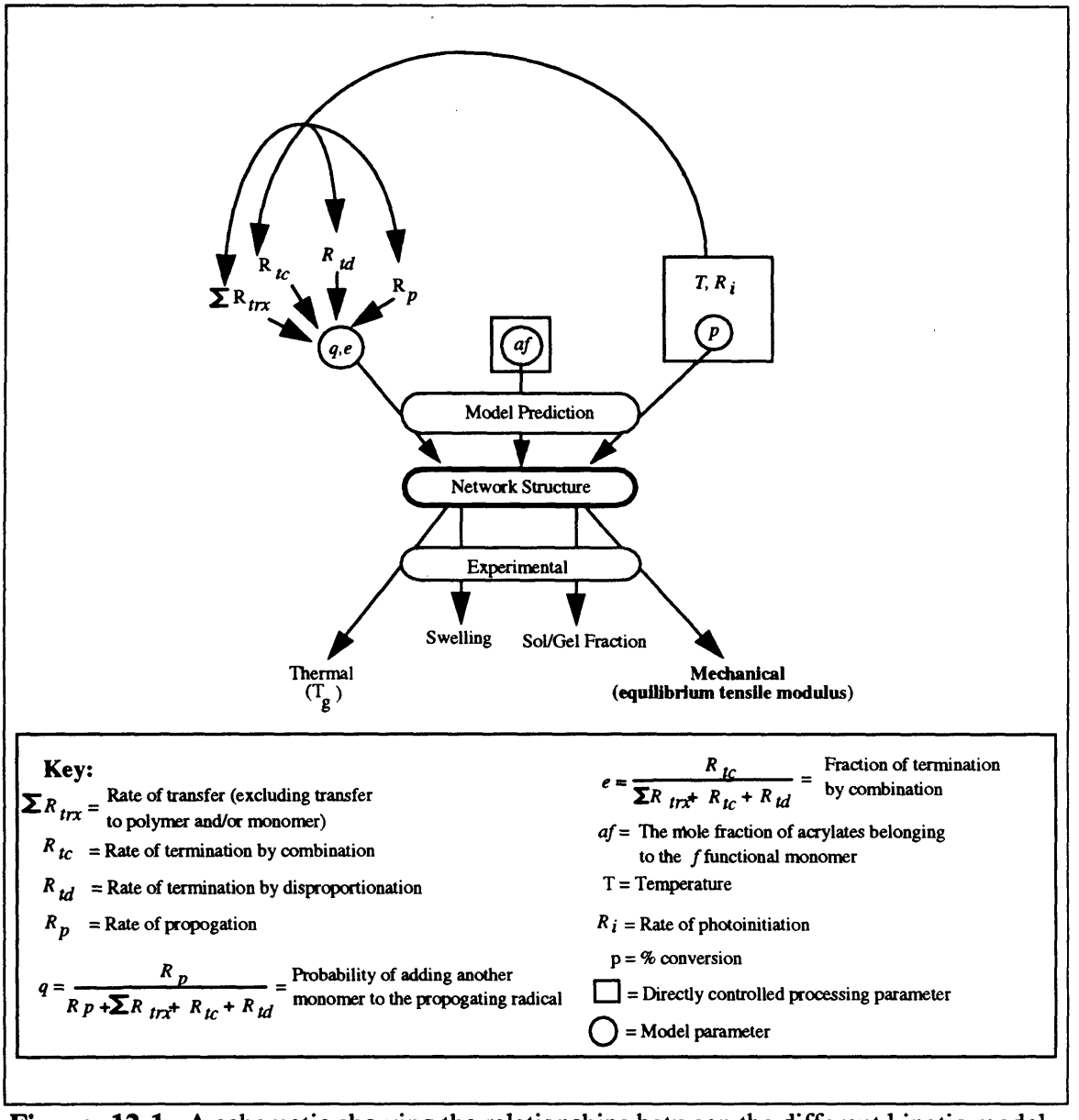

Figure -12-1. A schematic showing the relationships between the different kinetic model parameters and processing parameters which together predict the network structure and some of its respective structure-controlled macroscopic properties. This study focuses on equilibrium tensile modulus (under the ideal entropy elastomer assumption) as the primary crosslink density controlled macroscopic property. For a comprehensive treatment of The effects of crosslinking density on physical properties of polymers, see E.L. Neilsen's work.[6]

2.1 Modeling Polymer Network Structure Formation - An Historical Perspective

In an attempt to understand gelation phenomena, the concept of an "infinitely large molecule "was first developed by Flory in terms of a simple model proposed back in 1941.[7] Stockmayer followed with a more rigorous treatment using most probable size distributions in 1943-1944,[8,9] and ever since, the Flory/Stockmayer model (also known as the "classical theory") has served as the basis for a variety of statistical models developed up to this day. While many of these statistical models differ in their mathematical language, they all enjoy the simplicity of a mean-field theory by virtue of their being built upon the classical theory. In addition to general criticism against mean field theory as a whole, criticism of the statistical approach has centered around the inapplicability of theses models to describing structure development in kinetically controlled crosslinking polymerizations such as the free radical mechanism.[10] It is generally accepted, however, that for network forming polymerizations considered reacting in a thermodynamically controlled regime, statistical models provide a quite accurate description of the resulting structures. Examples of statistically based approaches include Gordon's theory proposed in 1962 which uses stochastic branching processes,[11] and the Macosko-Miller recursive model from 1976 which uses conditional probabilities.[12,13] In fact, a version of the latter model serves as the theoretical framework employed in this study. A more detailed discussion about the specific features of the model used here is provided in the next section.

Another class of models has been proposed with the advent of percolation theory (first introduced in 1957) which has opened a non-mean-field approach to the study of polymer network formation. Percolation models were enabled to develop with the explosive advancements in computer hardware and software during the past two decades.[14,15] These models are basically computer generated networks built on three-dimensional lattices. Simulations provide a detailed picture of polymer molecules, and structural information about the network is thus obtained. Presently, percolation theory is still very limited in its ability to account for complex molecular phenomena which control reaction characteristics.[4] That is why percolation theory has been mainly devoted to describe the network-forming polymerization near the gel point where system-specific features are less dominant in determining structure.

In 1988, Hamielec and Tobita started making a comprehensive contribution to what could be perceived as a third class of models designed to describe polymer network formation.[4,15,16,17,10] This new mean-field class embodies the so called kinetic approach which is designed to accurately account for the path dependent kinetics inherent in kinetically controlled polymerizations such as the free radical mechanism. Kinetic models involve the solution of differential equations describing concentrations of reactants while considering all important reactions in free radical polymerizations. An important feature of this method lies in its ability to demonstrate and calculate crosslinking[i] density distribution which is generally more difficult to account for in statistical approaches, and cannot be accounted for in classical statistical models due to the built-in assumption that all polymer chains have the same crosslink density. Of particular relevance to this study, however, is the fact that "the major weakness of [the kinetic] approach is its inability to provide information about the internal network structure such as the number of elastically active network chains."[18,19]

Despite on-going controversy as to which approach is the most accurate in, and appropriate for, describing network structure formation, it is also clear that each model has its merits and limitations. More importantly, however, it should be apparent that without sufficient experimental data in support of the usefulness of one model or another, the true assessment of the "truthfulness" expressed in any of the models might become somewhat irrelevant for purposes of potential applications. So while proposing theory for the sake of theory is valuable, there is at least as much value in proposing a theory for the sake of studying a particular simple model system by experiment. In this study, therefore, the emphasis lies in attempting to use one of the simpler models in conjunction with an appropriate experimental setup which would allow us to quantitatively describe network properties in terms of model predictions as well as explain deviations due to model limitations and characteristics specific to the experimental system.

[i] The definition of a crosslink in this context is merely a connection point between one growing chain to another, but this does not necessarily imply connectivity to the infinite network as is implied throughout this paper. This point will be later explained.

2.2 The Recursive Network Model as the Theoretical Framework

2.2.1 General

As a statistical approach based on the classical Flory/Stockmayer gelation theory, the recursive network model, originally introduced by Miller and Macosko [12,13] in 1976, is in essence equivalent to all other classical statistical approaches. Differences between these various statistical models can be found in their mathematical constructions and in the amount of obtainable information. It is the relative mathematical simplicity with which the recursive approach (and, similarly, Williams' recursive fragment approach)[20,21] obtains average structural parameters of the forming network that makes this model of particular applicability to this study in which we are mostly interested in the crosslink density of the gel as the average structural parameter dominating the thermo-mechanical behavior of entropy elastomers above T_g. Other important structural information obtainable from the model include number and weight average molecular weights, sol/gel fractions, gelation point, etc.

It is important to keep in mind the simplifying assumptions made by the particular version of the recursive model employed here. These assumptions may be of great significance in interpreting experimental results and rationalizing deviations form model predictions. In addition to the underlying free radical photo-polymerization mechanism assumptions which are discussed in the next section, the model employed as the theoretical framework of this study "retains Flory's ideal network assumptions:

1. All functional groups of the same type [,all acrylates in this case,] are equally reactive.
2. All groups react independently of one another.
3. No intramolecular reactions occur in finite species."[12]

It should be stressed that since its first introduction, several modifications have been included in later versions of the recursive model as well as in other mean-field approaches. Modifications were made in an attempt to accommodate a more realistic view of the kinetics of free radical polymerizations by accounting for the effects of structural distributions, relaxing some of the simplifying assumptions as those listed above, and considering additional reactions and deviations from the steady state assumptions. Among later versions (including the so called kinetic approaches) are models which account more

accurately for differences in modes of termination (combination vs. disproportionation),[22,20,21,23] models which account for cyclization [18,24,10,4] for depletion of monomer with conversion,[22] for differences in the reactivity between chemically distinct double bonds and radicals,[24,4] for dependence in reactivity between double bonds,[19,10,4] and for transfer to the polymer molecules.

In this study, we have avoided using the more complicated versions for several reasons. First, there is little advantage gained from using a model which accounts for a possible phenomena when there is no data to quantify it in terms of parameters to be used by the model. For example, since no data is readily available about the different reactivities of the double bonds (and certainly not as a function of temperature), one might as well assume that the reactivities are equal. Secondly, models which account for a more complicated kinetic reality, tend to be mathematically cumbersome and computationally difficult. Thirdly, when considering the fitting of data to model predictions, as more parameters are used in the fitting, conclusions may often be misleading due to mathematical artifacts. In conjunction with the relative simplicity of the chosen model, the experimental setup in this study was designed to accommodate to the best approximation the simplifying assumptions imposed by the statistical model. The idea in this setup is to maximize the potential gains from the simplicity of the model while minimally sacrificing the reliability of the model in interpreting experimental data.

2.2.2 The Model Itself

Figure 2-1 provides a schematic of the statistical model and its function within the overall scheme of this study. The model takes as input the composition of the monomers or network building blocks, the degree of conversion, and two kinetic parameters (q and e), which are functions of the free radical rate parameters. The output produced by the model is a group of average structural parameters of the polymerized gel or network, depending on the conversion level and the gelation point, which is also derived in the model. Despite the conceptual simplicity of the probability and statistics employed in producing the model's output, the equations to be solved in the process often require numerical solutions.

An understanding of model implications represented by the q, e, p, and af parameters provides useful insight on the directions in which each of these parameter can affect the network structure. This information will be particularly important later on when

discussing ways in which changes in temperature, photo-initiation rate, formulation, and conversion affect the resulting network structure. Parameters q, e p, and af are all defined between 0 and 1, and can be viewed as probabilities. Expressions for each of the parameters are given in the key of **Figure 2-1.** Parameter p represents the overall level of conversion, or simply the probability that any reactive group within either the sol or gel fractions, has reacted. Parameter q is the probability that a propagating radical will add another monomer unit to the chain. As expected, q approaches 1 if $R_p >> \sum R_{trx} + R_{tc} + R_{td}$. That is, termination and transfer rates are minute relative to the propagation step. Parameter e is the probability that the killing of a radical takes place by combination rather than by disproportionation or by transfer.[ii] Parameter e approaches 1 as $R_{tc} >> \sum R_{trx} + R_{td}$. That is, combination becomes the dominating radical "killing" process. Qualitatively, it should be apparent that the closer q and e are to 1, the longer the individual propagating chains, and thus, the higher the connectivity and crosslink density of the resulting network.

Parameter af is a formulation parameter. Though in theory the recursive analysis can be extended to study structures of any multi-component system, the particular version used here is designed for a two-component system in which one component is mono-functional and the other is of any functionality, f. In our case study of a monoacrylate/diacrylate system, under the equal reactivity assumption, af can be interpreted as the probability that a reacted acrylate group belongs to the diacrylate rather than monoacrylate monomer (af = 2[diacrylate] / (2[diacrylate] + [monoacrylate]). Parameter af will approach 1 as we increase the diacrylate concentration up to the point where we end up with a single component difunctional system. In this study, we chose a two-component system and, for the most part, keep the components' respective concentrations constant. One should realize, however, that for any system, as one increases the relative concentration of the reactive groups belonging to the higher functionality components keeping other factors constant (causing af to approach 1 in our two-component system,) a more highly crosslinked network develops. More will be discussed about q, p, e and af in Section 2.6.1.

[ii] A dead chain is defined here as either a terminated chain, (by combination or disproportionation), or as the result of transfer of a chain radical to another monomer. Thus, "killing" a radical would either be terminating it or transferring it.

2.3 The Free Radical Kinetics of the Study Model System

Though the statistical model employed in this study is powerful in predicting network structure for a given set of free radical kinetic parameters (R_{trx}, R_{tc}, R_{td} and R_p as shown in **Figure 2-1**), and given conditions satisfying its assumptions, in order to understand the effects of changing curing temperature, initiation rate, and degree of conversion on the resulting network structure, we must first establish the underlying relations between these variables and the kinetic parameters. These relationships, expressed by the four top arrows of **Figure 2-1**, and the interactions between the different rate parameters are expressed through their respective step rate constants and based on the steady state assumptions of the free radical photopolymerization mechanism as used in this model.[iii] The implications of the free radical kinetics on the particular model system and reaction conditions used in this study are summarized in Sections 2.3.1 - 2.3.5.[25,26,27]

2.3.1 Initiation

The photo-initiation process is considered fixed by the concentration of initiator and the irradiation spectra and intensity. This process is assumed to be independent of temperature for purposes of studying crosslink density changes with polymerization temperatures in the range explored in this study.[28] R_i is taken as a constant throughout the polymerization reaction, which consumes a negligible amount of the starting concentration[iv] **Equation 2-1** gives the photo-initiation rate (molar/s) as a function of UV intensity, the efficiency of chain initiation (Parameter F), and a constant, K, which is the integral sum of the initiator's spectral photonic absorption in moles/(cm Joule). K and F are functions of the particular photo-initiator and its surrounding environment only, and thus are expected to remain sufficiently constant within the polymerization temperature range of the study in order to satisfy the temperature independence of R_i within an acceptable level.

$$R_i = 2F \cdot I_0 \cdot K \qquad \textbf{(2-1)}$$

[iii] Specifically there is no account for conversion dependent kinetics (monomer depletion). Instead the average monomer concentration is used (defined as the concentration at 50% of the conversion level of interest). As for the statistical model itself, no account is taken for transfer to either the monomer or polymer though they are accounted for in the general kinetics.

[iv] R_i is also assumed independent of conversion in the sense that F is sufficiently independent of conversion. This may not always be the case is shown in Ref. 32 which discusses the "cage effect".

An expression for K is provided in **Appendix A.** The factor of 2 in **Equation 2-1** represents the assumption that the two radicals, (chemically distinct in our case), generated by the splitting of the initiator molecule upon photon absorption, are sufficiently equally reactive at all temperatures of the study. Note that R_i is directly proportional to the irradiation intensity, a "processing parameter, "which is relatively easy to control.

2.3.2 Termination

The steady state assumption equates the rates of initiation and termination by both combination and disproportionation. This equation is used to calculate the steady state radical concentration. **Equation 2-2** introduces K_t, the termination step rate constant, which is the sum of K_{tc} and K_{td} the rate constants for termination by combination and disproportionation, respectively. The termination rate for either mechanism is second order in radical concentration.

$$R_t = 2 \cdot K_t \cdot [\mathrm{M}\bullet]^2 = 2 \cdot (K_{tc} + K_{td}) \cdot [\mathrm{M}\bullet]^2 = R_i \qquad \textbf{(2-2)}$$

where [M •] = concentration of free radicals

2.3.3 Propagation

R_p, the propagation rate, is first order in both the steady state radical concentration and monomer concentration. K_p is the rate constant for the propagation step. Using [M •] from **Equation 2-2**, one derives the expression for R_p as a function of initiation rate, monomer concentration, and the kinetic constants as shown in **Equation 2-3.**

$$R_p = Kp \cdot [\mathrm{M}\bullet] \cdot [\mathrm{M}] = \frac{K_p}{(2K_t)^{1/2}} R_i^{1/2} (1-p)[\mathrm{M}]_0 \qquad \textbf{(2-3)}$$

2.3.4 Transfer Reactions

Possible transfer reactions that generally need to be considered in a bulk polymerization include transfer to the monomer, to the polymer, to the photo-initiator, and to other unknown low-concentration-impurities that may act as effective transfer agents. Naturally, the cases of transfer to the monomer and/or to the polymer are the more complicated ones in terms of their implications on the resulting network structure.[v] From

[v] Qualitatively, for any fixed conversion level, kinetic chain length, and termination fraction by combination, transfer to the monomer and/or polymer is expected to reduce the overall crosslinking density for a system in which crosslinkers are present (such as the one employed in this study). This effect is associated with changes in the molecular size distribution which is expected to become narrower with

the free radical kinetic perspective, however, all transfer reactions are treated in the same general manner as expressed in **Equation 2-4**, where [X][vi] is the concentration of the transfer agent, and K_{trx} is the respective transfer rate constant.

$$R_{trx} = K_{trx}[M\bullet][X] \qquad \textbf{(2-4)}$$

In the case of transfer to the monomer, for example, we get an expression analogous to the propagation rate which is first order in radical and monomer concentrations. This is shown in **Equation 2-5**, where K_{trm} is the transfer to monomer rate constant.

Implicit in **Equation 2-3** in which R_p is independent of transfer reactions, is the assumption that the initiation of a new propagating chain following transfer to any species is at least as fast as the rate of propagation of the radical.

$$R_{trm} = K_{trm}[M\bullet][M] = K_{trm}[M\bullet](1-p)[M]_0 \qquad \textbf{(2-5)}$$

A priory, in the system considered here, one may choose to neglect the importance of transfer to the initiator considering the instability of high-energy photo-activated radicals formed during initiation, and the low photo-initiator concentration.[vii] Transfer in general, however, can be most dominant in controlling the polymerizing network structure, even when disguised in the overall observed kinetics.

So, while transfer may not necessarily affect the overall polymerization rate, it often significantly affects the degree of polymerization, D_p, an average kinetic quantity expressed in **Equation 2-6**. The second term on the RHS of this equation (in parentheses following the third and fourth "=" signs) represents the inverse of the kinetic chain length (denoted υ), which by definition equals R_p/R_i (= number of molecules consumed per chain started). Parameterω, expressed below, represents the probability that given a randomly

---

any transfer including to the monomer and/or polymer. Obviously, for an otherwise linear system, transfer to monomer and/or polymer in the presence of sufficient termination by combination will increase the crosslink density (to above the 0 level of any linear system irrespective of its degree of polymerization.) Any quantitative theoretical treatment of the effects of transfer to monomer and/or polymer on network structure development are beyond the scope of this study. For more detail, see Ref. 23.

[vi] Which, again, for purposes of predicting the crosslink density via the statistical model, does not include the monomer and/or polymer.

[vii] A low initiator concentration is generally not a sufficient condition for neglecting the possibility of significant transfer even for concentration < 0.1 wt%.

chosen dead chain, the chain would have been formed by combination rather than by transfer or disproportionation.[viii]

$$\frac{1}{D_p}=\frac{1-q}{q\omega}=\left(\frac{\Sigma K_{trx}[X]+(2K_t R_i)^{1/2}}{K_{tp}(1-p)[M]_0}\right)\frac{1}{\omega}=\left(\frac{\Sigma K_{trx}[X]}{K_{tp}(1-p)[M]_0}+\frac{1}{\upsilon}\right)\frac{1}{\omega} \qquad \textbf{(2-6)}$$

Where $\omega=(\gamma(2\delta-1)+1)$ in which $\delta=\dfrac{1+\frac{K_{td}}{K_{tc}}}{1+2\frac{K_{td}}{K_{tc}}}$ and $\gamma=\dfrac{1+\frac{K_{tc}}{K_{td}}}{1+\frac{K_{td}}{K_{tc}}+\frac{\sqrt{2K_t}\Sigma K_{trx}[X]}{R_i^{1/2}K_{tc}}}$

2.4 Temperature and Initiation Rate Effects on the Free Radical Step Rates

While the kinetic effects caused by changing the initiation rate are relatively straight forward as one can see from the above relations, the effects associated with changing the polymerization temperature are far more complicated. In the following discussion we will stick to our earlier assumption that R_i, the photo-initiation rate, is sufficiently independent of the reaction temperature. First, lets consider the more simple case of changing R_i only.

2.4.1 Initiation Rate Effect

The rate of termination, R_t, which by the steady state assumption equals R_i, will obviously change proportionally to R_i. From **Equation 2-3** we see that the overall propagation rate is directly proportional to the square root of the initiation rate. The quantity R_p/R_i, (defined as the kinetic chain length, ν) will vary proportionally to $1/R_i^{1/2}$. This result can be seen in **Equation 2-6**, which gives D_p as a function of R_i and ω. Upon substitution of an R_i-dependent expression for ω (see **Equation 2-6**), one realizes that the initiation rate effect can change γ (and therefore,ω) by a maximum factor of 2 for the limiting case of $K_{tc}>>K_{td}$ ($\delta=1$).

Therefore, despite the apparent complexity of **Equation 2-6**, for any practical purposes, the relationship between D_p and R_i is relatively simple. Predominantly, D_p will change due

[viii] $(1-\gamma)$ represents the fraction of radical killing events taking place by transfer. δ represents that fraction of terminated radicals by combination. By separating between the cases of transfer and (bimolecular) termination, and by accounting for the probability of combination (for the termination case), one derives combination ω which is the probability that a randomly picked killed chain has been formed by combination (and is therefore on average twice the size of chains resulting from transfer transfer or disproportionation.

to changes in q since ω can only vary between 1 and 2, and thus, the maximum effect of ω would be to change D_p by a factor of 2. In the case of negligible transfer, D_p will vary in direct proportion to $1/R_i^{1/2}$, which is expected since D_p and ν will differ only by the ω factor (which further means that they will be equal to one another as K_{tc} approaches 0.) In principle, for cases in which transfer cannot be ignored and $K_{tc}>0$, changes in R_i would cause opposing effects on D_p through q and ω which change in opposite directions as a function of R_i. An interesting case occurs when ω dominates. This case is unrealistic, but mathematically possible under conditions of $\Sigma K_{trx} >> K_p >> (R_i)^{1/2}$, and $K_{tc} >> K_{td}$. Under these conditions, $D_p << 1$, and therefore the case is physically meaningless for our purposes.

For the real system, D_p will always decrease with increasing R_i, and the percentage change in D_p will depend on the relative magnitudes of the two terms making q. The larger the first term is relative to the second, or the more significant transfer is, the smaller will be the change in D_p as a function of R_i. It is important to realize, however, that a small percentage change in D_p can cause a greater percentage change in the crosslink density, (and therefore in the modulus), of a nonlinear system than a larger percentage change in D_p. The condition for this to happen requires that one starts with a small enough D_p, which would naturally be the case the larger transfer and the lower the rate of propagation. In other words, the effect of R_i on the crosslink density can be more dramatic at a low D_p even though D_p may change by a relatively small percentage for small D_p values. This point will be demonstrated when considering the direct effects of R_i and T on the crosslink density by use of the statistical model.

2.4.2 Temperature Effect

Temperature affects the individual reaction rate of the steady state free radical kinetics through the respective rate constants. The simultaneous changes of at least four different rate constants (K_{tc}, K_{td}, K_p, K_{trx}) in addition to possible activations of other physico-chemical processes outside those encompassed by the free radical model, make the study of temperature effects on the overall reaction extremely complex. The rate constants are commonly treated as Arrhenius expressions with a single activation energy corresponding to each of the individual rate processes. As a first approximation, in order to predict the effect of temperature on the overall reaction kinetics, one can plug the Arrhenius expressions with their built-in temperature dependence into each of the equations provided above for the corresponding free radical polymerization steps. The activation processes are thus considered constants with respect to temperature in this treatment. It is readily

noticed from the expressions below that propagation and transfer rates as well as changes in the modes of termination with temperature depend in this model on the relative magnitude of the different constant activation energies. Furthermore, the response of D_p to changes in temperature incorporates all of these simultaneous variations.

Since the free radical mechanism is assumed to hold at all temperatures studied, and since we have assumed that R_i is independent of temperature, we have to conclude that the R_t ($=R_{tc}+R_{td}$) is also kept constant with temperature. The relative fraction of termination by combination versus termination by disproportionation may change with temperature depending on the respective activation energies as shown in **Equation 2-7**. The total rate termination, however, which is the sum of the two termination processes, is kept constant with temperature.

$$\text{Fraction of termination by combination} = \frac{R_{tc}}{R_{tc}+R_{td}} = \frac{1}{1+\frac{A_{td}}{A_{tc}}e^{\frac{-(E_{td}-E_{tc})}{RT}}} \qquad \textbf{(2-7)}$$

As polymerization temperature rises, the rate of termination by combination increases at the expense of a decrease in the disproportionation rate if $E_{tc}>E_{td}$. **Equation 2-8** gives the rate of propagation as a function of temperature. A sufficient condition for increasing the rate of propagation with temperature is $E_p>1/2$ (the larger between E_{tc} and E_{td}) assuming $A_{td}=A_{tc}$.

$$R_p = \frac{A_p R_i^{1/2}(1-p)[\mathrm{M}]_0}{\sqrt{2A_t}}\left(A_{td}e^{\frac{-(2E_p-E_{tdp})}{RT}}+A_{tc}e^{\frac{-(2E_p-E_{tc})}{RT}}\right)^{1/2} \qquad \textbf{(2-8)}$$

Plugging the rate steps into **Equation 2-6** results in the complicated expression for D_p given in **Equation 2-9**.

$$D_p = \frac{(\gamma(2\delta - 1) + 1) A_p (1-p)[M]_0}{\Sigma\left(A_{trx}[X] e^{\frac{-(E_{trx} - E_p)}{RT}}\right) + \sqrt{2} R_i^{1/2} \left(A_{td} e^{\frac{-(E_{td} - 2E_p)}{RT}} + A_{tc} e^{\frac{-(E_{tc} - 2E_p)}{RT}}\right)^{1/2}}$$

$$\text{Where } \delta = \frac{1 + \frac{A_{td}}{A_{tc}} e^{\frac{-(E_{td} - E_{tc})}{RT}}}{1 + 2\frac{A_{td}}{A_{tc}} e^{\frac{-(E_{td} - E_{tc})}{RT}}} \qquad \textbf{(2-9)}$$

$$\text{and } \gamma = \frac{1 + \frac{A_{td}}{A_{tc}} e^{\frac{-(E_{td} - E_{tc})}{RT}}}{1 + \frac{A_{td}}{A_{tc}} e^{\frac{-(E_{td} - E_{tc})}{RT}} + \frac{\sqrt{2}}{R_i^{1/2} A_{tc}} \Sigma A_{trx}[X] \left(A_{td} e^{\frac{-(2E_{trx} + E_{td} - 2E_{tc})}{RT}} + A_{tc} e^{\frac{-(2E_{trx} - E_{tc})}{RT}}\right)^{1/2}}$$

As expected, the same inequalities that increase the rates of propagation and termination by combination, would also tend to increase D_p with increasing temperature. However, **Equation 2-9** demonstrates some of the complexities that arise from the simultaneous changes in four different temperature dependent terms. Naturally, studying the effects of temperature on the resulting network structure in nonlinear systems, complicates the picture even further, especially when some of the free radical assumptions and simplifications need to be relaxed. **Equation 2-9** gives the following inequalities as independent conditions that would each contribute to increasing the D_p with increasing polymerization temperature (assuming A_{td}=A_{tc}): $E_p > E_{trx}$, $E_p > 1/2$ (the larger between E_{tc} and E_{td}), $E_{trx} < 1/2$ (the smaller between ($1/2E_{td} - E_{tc}$) and $1/2E_{tc}$), $E_{tc} > E_{td}$. Theoretically, satisfaction of all four conditions is sufficient for D_p to be strictly increasing with temperature. However, and as will be stressed later on, the third and fourth inequalities which would together change D_p by a factor of two at most, can be disregarded as important factors under rather usual conditions.

2.5 From Linear to Nonlinear Systems - An Intuitive Perspective

Understanding variations in D_p as a function of R_i and T for a given linear system enables us to apply similar principles in this study of a nonlinear system. In fact, one can establish a relationship between the structural representations embodied by D_p and the crosslink

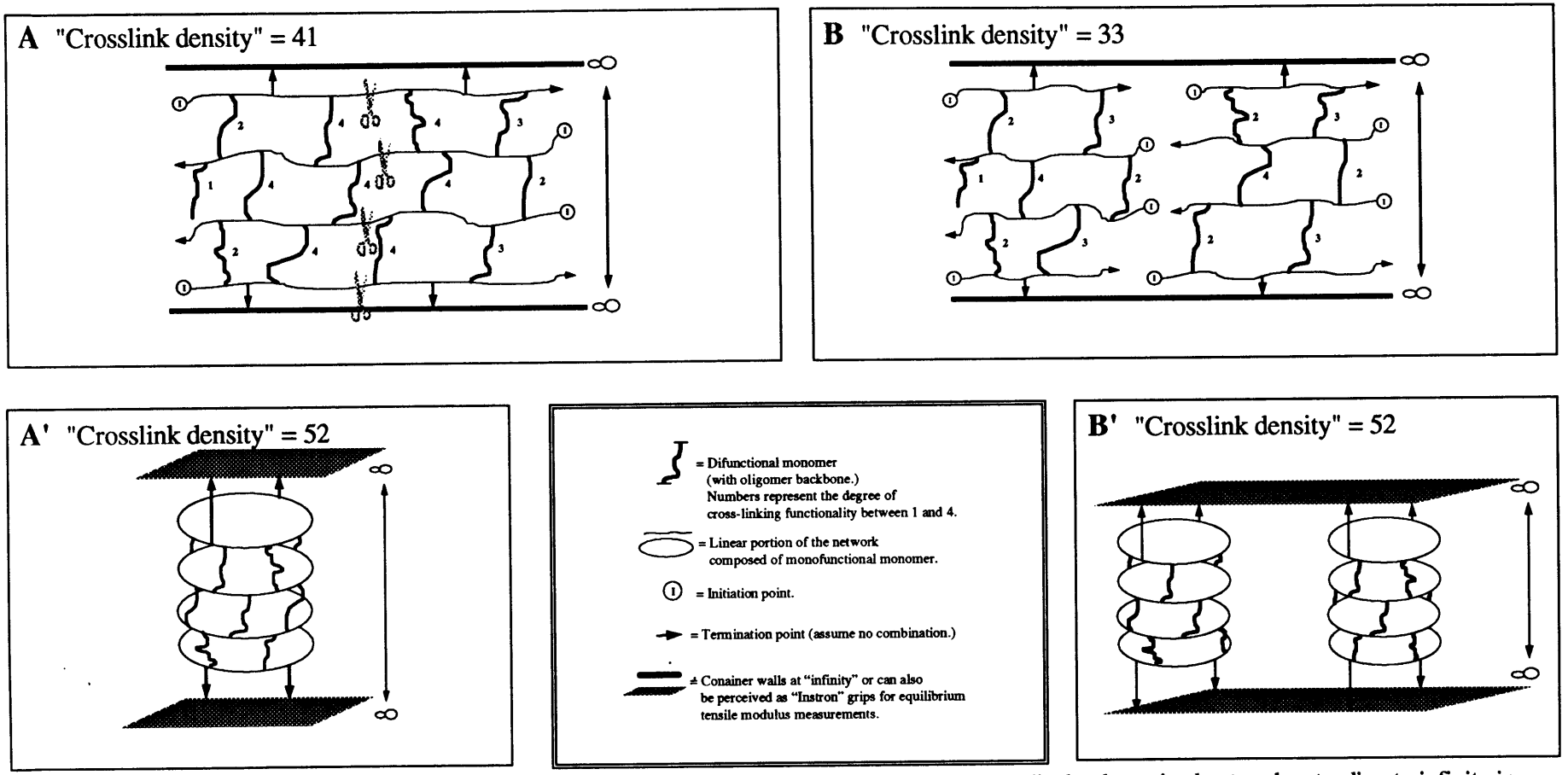

Figure 2-2. Network A represents an idealized two-dimensional, monofunctional/difunctional, free-radical polymerized network extending to infinity in the vertical dimension only. Network B is the result of cutting four chains from Network A. As a result, Network B has eight less effective links than network A. Though unrealistic according to the recursive model, in this idealized schematic one can perceive Network B as having an average chain length that is half that of A. Networks A' and B' are the respective perfect networks in which each of the difunctional monomers serves as a four functional crosslinker. Keeping in mind that "infinity" is still defined in the vertical dimension only, A' and B' have the identical number of maximum possible crosslinks, 52. Creating B' from B required eight more links than were necessary in creating A' from A.

density parameter for linear and non-linear systems, respectively.[ix] In this model, D_p and the crosslink density are both functions the same rate parameters of the free radical polymerization mechanism regardless of the linearity or non-linearity of the system. It was already shown that the greater ν and *e*, and the smaller R_{tr}, the greater D_p, which means the longer is the average chain length of a linear system. Considering a nonlinear system like the one used in this study, the greater D_p, the more crosslinking units are incorporated per chain between its initiation and termination points. This is because, statistically, as the chain propagates, a crosslinking unit (a diacrylate in this case) is incorporated between every fixed number of the other monomers units (monoacrylate in this case). Put differently, for a given mass, a statistical network with a higher average chain length[x] will have proportionately less chain ends[xi] as can be shown in the simple **Equation 2-10**. Each time we introduce a break in a chain within the network, we introduce two chain ends and as a result we loose two links per every additional chain break.[29] In other words, there is a link lost for every additional chain end created. Whenever a destroyed link had served the network as an effective crosslink, the crosslinking density will decrease.

$$\#\text{ of chain ends} = 2\frac{\#\text{ of monomers in the network}}{\text{Average chain length}D_p} \qquad \textbf{(2-10)}$$

For demonstration, lets consider a highly idealized two-dimensional network whose building blocks are as in our actual case study, a monofunctional and difunctional monomer. See **Figure 2-2**.

[ix] For example, it has been shown that $Dp = (q\omega/(1-q))$, and similarly, D_p can be directly calculated as a function of *q* and *e* only (see Refs. 11, 19, 20 for the degenerate cases). Therefore, under the assumptions of the statistical model, one can estimate the crosslink density as a direct function of D_p. For fixed q or e (so that D_p is strictly a function of only one of these parameters) an "exact" relationship between D_p and the CLD can be established. For the sake of completion, it should be mentioned that for a given D_p, a high-*q*-low-*e* system is predicted by the statistical model to give a higher crosslink density at any conversion and af relative to a high-*e*-low-*q* system. This finding is rather irrelevant for any practical purposes in this study, and in the general case in which the effect of e relative to q in determining D_p (and therefore the crosslink density) is negligible. At low enough q values and low enough R_{tr}/R_i, the difference due to the q/e composition effect (for a given D_p, *af*, and conversion) may become significant. A qualitative argument to rationalize the *q/e* composition effect is that it controls the distribution around D_p (combination narrows this distribution) so that for high-*q*-low-*e* systems, the crosslink density gains from an "exponential type" increase in the crosslink density with an increasing fraction of the longest chains.

[x] The term "average chain length," as opposed to D_p, is used intentionally to reflect the idea that we are considering here the network as a complete structure without considering realistically the kinetics that would be required to "design" a particular network structure.

[xi] Chain ends in the context of a network are defined as those parts of the chain which do not connect **back** to the "infinite network structure."

For simplicity, lets assume that the network is infinite[xii] only in the vertical dimension. Networks **A** and **B** in the figure represent the same "conversion level"[xiii] that is they are composed of the same number of mono and difunctional groups respectively. The distance along the chain between each pair of neighboring crosslinkers is normally distributed around an average equal to $(1-af)/af$ units of monofunctional monomers following the equal reactivity assumption. Although the network schematics of **Figure 2-2** would generally be considered improbable according to the recursive model, for high enough D_p and conversion levels, one can think of Network A as simply having a D_p which is twice that of Network B. More realistically, one can imagine breaking each one of the four chains of Network A in order to create Network B, which would therefore have twice the number of chains and twice the number of chain ends compared to A.

Since each f-functional group is capable of connecting to the infinite network via $2f$ chain extensions or arms, it has a maximum crosslinking capability of functionality $2f$. Thus, a difunctional group such as a diacrylate can serve as either a four or three functional crosslinker. In the case of only two of its arms leading to the infinite network ("two functional crosslinker") it would only be a part of a chain or a link. If only one of its arms is connected to infinity ("1 functional linker"), it would be considered a dangling chain. Using this scheme for counting crosslinks[xiv] (or more accurately, links), one can sum up the total crosslinks for all difunctional groups in each network to find that Network A has exactly eight crosslinks more than Network B. This result is expected since four chains have been broken in creating Network B from A.

Another way of illustrating the implications of D_p is to consider the perfect network. **Figures 2-A'** and **2-B'** are perfect three dimensional networks in which each difunctional group has exactly four arms extending to infinity and each monofunctional group has exactly two arms extending to infinity. In both cases, the perfect network is created by connecting the initiation and termination points of each chain, and by connecting dangling

---

[xii] Infinite means that the network extends to both horizontal walls of its container or as illustrated here, to the upper an lower grips of an "Instron" used for measuring tensile equilibrium modulus.

[xiii] More correctly, we should say that they are composed of the same mass. In a realistic model it is impossible that two infinite networks developing with different average D_p values, will have exactly the same composition at the same level of overall conversion. However, as we consider high conversions and high enough D_p values, the overall conversion level would approximate the network mass.

[xiv] A different scheme for counting the cross-links is introduced later when defining effective crosslinks for purposes of modulus predictions according to a model and based on the actual monomer formulation used in this study. Both counting schemes, however, result in the same difference of eight crosslinks between the two networks.

chains into any point in the network. Networks A' and B' have the same number of maximum crosslinks and, thus, are equivalent for purposes of counting the number of effective entropy springs in each network. However, the difference between the cases is that while creating network B' from B required only six (4+2) additional bonds, creating A' from A required ten (8+2) additional bonds. So the difference of exactly four bonds (or eight crosslinks) shows up again. This idealized and unrealistic example demonstrates the importance of the ratio $D_p^{network\ A} / D_p^{network\ B}$ in comparing the crosslink densities of two given networks. We can express this more quantitatively as a relationship that would hold for purposes of comparing any two network systems having the same monomer formulation, density, and degree of conversion.

$$\Delta\ Crosslink\ Density = \frac{2\rho}{D_p^{networkA}}\left(1 - \frac{D_p^{networkA}}{D_p^{networkB}}\right) = 2\rho\left(\frac{1}{D_p^{networkA}} - \frac{1}{D_p^{networkB}}\right) \qquad \textbf{(2-11)}$$

Where ρ is the reactive group (acrylate) density (moles / unit volume)

Equation 2-11 is naturally an underestimate of the real change in the crosslink density for more realistic networks developed according to the recursive model. **Figure 2-3** on the following page compares the idealized approximation as expressed by **Equation 2-11** to the statistical model prediction. The figure shows the absolute value of the predicted crosslink density reduction relative to $D_p = 1000$. Qualitatively one notices for both predictions the strong exponential type of increase in the crosslink density difference as D_p becomes smaller (the difference approaches the crosslink density at $D_p = 1000$ as D_p approaches 1.) Quantitatively, however, it is clear that the idealized model prediction is valid only for very large D_p values as earlier stated, and that the ideal model dramatically underestimates the crosslink density difference resulting from reducing D_p to smaller values.

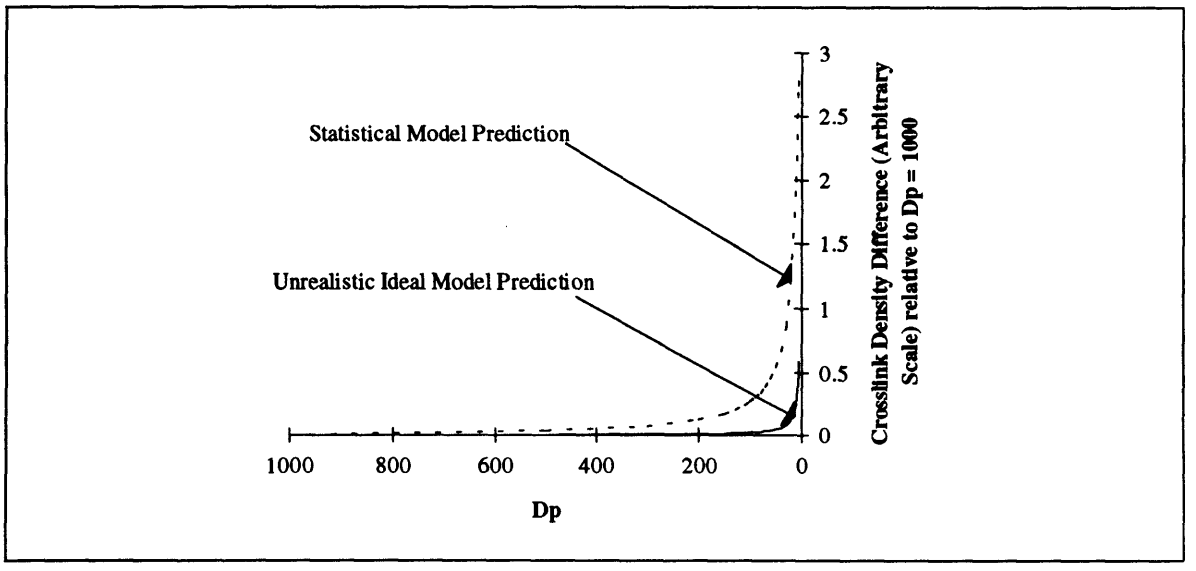

Figure 2-3. Comparison between the unrealistic ideal model prediction and the statistical model prediction (both calculated for arbitrarily chosen e=0 and af=0.189) giving the absolute value of the full conversion reduction in the crosslink density as a function of D_p, relative to D_p=1000.

Though the above approach of drawing analogies between linear and nonlinear structures is an important tool for developing an intuitive grasp of the underlying relations between the free radical kinetics and the resulting network structure, it is rather limited in providing a more detailed quantitative statistical description of structure as function of conversion. We still need, however, to understand how changes in T and R_i which are taken as constants for a given non linear polymerization, affect the resulting different network structures for any fixed level of conversion.

2.6 Applying the Model as a Predicting Tool

The statistical model is "blind" to the direct influence of R_i and T. It considers only e, q, and af as direct parameters that control the network structure for a given conversion level, p. The first step, therefore, in studying network structure control via the processing and formulation parameters is to simulate model predictions as a function of e, q, af, and p. Once these relations are understood, we need to focus our attention on manipulating q, e, and p via control of R_i and T, and while choosing an appropriate af for the given chemistry. When keeping in mind industrial applications, control of q, e, and p does not only mean choosing their optimal levels, but also assuring that expected drifts from these

optimal values would not change the network properties in a significant manner. In other words, the ideal system should be robust enough to accommodate expected fluctuations in the processing parameters so that the desired structure-related network properties of the product are minimally affected.

2.6.1 Model Predictions of Crosslink Density as a Function of *q*, *e*, *af*, *p*

2.6.1.1 Appreciating the Influence of Parameter *e* on the Crosslink Density

The maximal absolute difference in crosslink density between any two curves of fixed q and af giving crosslink density as a function of conversion, is located at p=1, or at full conversion. Thus, in order to get an upper limit value on the absolute differences in crosslink density predicted by the model for a complete shift in the termination mechanism (100% combination to 100% disproportionation or vice versa) under different conditions, model predictions are calculated for p=1 and presented in **Table 2-1** on the following page. The representative cases considered consist of all combinations of full conversion polymerizations under a series of different q and af values, and for a series of R_{tr}/R_i ratios.

In general, q is not independent of R_{tr}/R_i, however, the two quantities are artificially presented as such in the table for the sake of deductive arguments. Also, in calculating the crosslink density, q was taken as constant throughout the polymerization reaction, even though q is decreasing with the depletion of monomer. Since in many cases q can be taken as a constant quantity, and since the following analysis is identical when accounting for monomer depletion, it is unnecessary to deal with the associated computational complications.

The importance of the R_{tr}/R_i ratio in controlling the influence of switching termination mechanisms on crosslink density is indirect via control of e as one can see from its

Table 2-1

The Effect of the Termination Mechanism on the Crosslink Density

P	*af*	R_{tr}/R_i	*q*	100% Disproportionation		100% Combination		Absolute Difference	% Difference (Crosslink Density is "100%" for 100% disproportionation)
				Predicted Crosslink Density (arbitrary unitless scale)	*e*	Predicted Crosslink Density (arbitrary unitless scale)	*e*		
1	0.25	0	0.90	2.45	0	3.86	1	1.41	57.5
			0.95	4.06		4.99		0.93	22.9
			0.999	6.16		6.19		0.03	<1
		10	0.90	2.45		2.58	0.091	0.13	5.3
			0.95	4.06		4.14		0.1	2.4
			0.999	6.16		6.17		0.01	<1
		100	0.90	2.45		2.42	0.0099	0.02	<1
			0.95	4.06		4.07		0.01	<1
			0.999	6.16		6.16		0	<1
	0.20	0	0.90	1.45		2.57	1	1.12	77.3
			0.95	2.77		3.57		0.8	28.9
			0.999	4.66		4.69		0.03	<1
		10	0.90	1.45		1.55	0.091	0.1	6.3
			0.95	2.77		2.84		0.07	<1
			0.999	4.66		4.67		0.01	<1
		100	0.90	1.45		1.46	0.0099	0.01	<1
			0.95	2.77		2.78		0.01	<1
			0.999	4.66		4.66		0	<1
	0.15	0	0.90	0.62		1.38	1	0.76	123
			0.95	1.58		2.23		0.65	41
			0.999	3.23		3.25		0.02	<1
		10	0.90	0.62		0.68	0.091	0.06	9.7
			0.95	1.58		1.64		0.06	<1
			0.999	3.23		3.23		0	<1

expression. As shown in **Table 2-1**, as R_{tr}/R_i increases to 100, e is constrained between 0 and 0.01, and, as a result, the crosslink density is essentially independent of the termination mechanism even for q values as low as 0.9. For lower R_{tr}/R_i ratios, changes in termination mechanisms can change e between 0 and as high as 1 for the case of no transfer. Nevertheless, a high enough q value can dampen the effect of a change in e between 0 and 1, and offers another regime where the crosslink density is effectively independent of the termination mechanism. From the table, one can also conclude that af (in the range considered) has the weakest influence on the crosslink density difference, though qualitatively, the absolute difference value decreases as af decreases.

The conditions under which changes in the termination mechanism significantly affect the crosslink density are sufficiently small q and R_{tr}/R_i values. In a more realistic analysis, for a given rate of initiation, as the rate of transfer increases, q decreases while R_{tr}/R_i increases. These two changes will have opposing effects on the influence of the termination mechanism. Generally, however, considering low enough initiation rates, the presence of reasonable transfer will restrict e to values close to 0 while q will be dominated by the R_{tr}/R_p term. Since R_{tr}/R_p is normally $<<1$, in the most common case the termination mechanism, or e, has a negligible influence on the crosslink density.

It should be pointed out that when considering the % changes in crosslink density between disproportionation and combination as shown in **Table 2-1**, one notices a significant increasing trend as af decreases for a given q and R_{tr}/R_i values. An increase in the % change would also be noticed with decreasing conversion levels. Though this fact might be important for practical application purposes, in this study we focus most attention on the high conversion regions and af values around 0.2 and above. This is partly because modulus measurements in the experimental setup are more sensitive to absolute differences which increase with increasing conversions and af values. In any case, it is clearly shown that overall, the influence of the termination mechanism even when measured in % change of crosslink density is primarily dominated by the R_{tr}/R_i ratio and by q so that in a realistic system at relatively high conversions the af effect on the % difference due to changing termination mechanisms can still be ignored.

2.6.1.2 Appreciating the Influence of Parameter q on the Crosslink Density

Two aspects of q as a factor determining crosslink density need to be discussed. First, as can be seen from **Table 2-1**, for a fixed af value and conversion level, q has a strong effect

on the crosslink density irrespective of the termination mechanism, or *e*. Secondly, when considering crosslink density as a function of conversion, *q* has a significant effect on the curvature of this relationship. **Figure 2-4** illustrates important features in the relationship between *q*, *p* and the crosslink density which is represented as the fraction of the theoretical maximum crosslink density. The latter quantity is strictly controlled by the concentration of crosslinking unites, or *af*. More will be discussed about counting effective crosslinks with relation to modulus predictions in the experimental section.

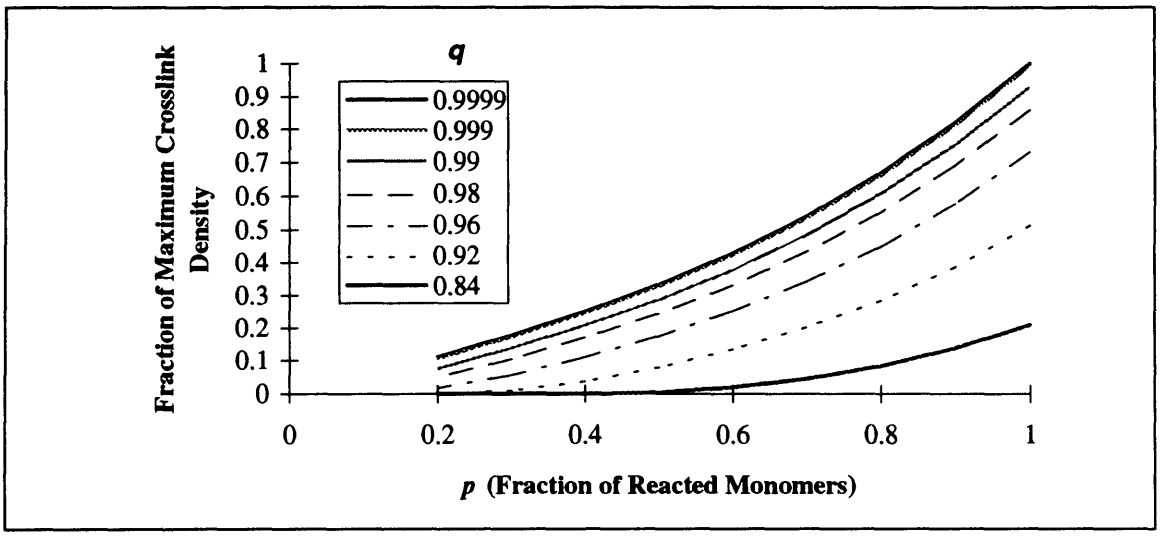

Figure 2-4. Predicted fraction of maximum crosslink density as a function of conversion for different *q* values. Calculations were made for *af*=0.15 and *e*=0.5.

As *q* approaches unity, the crosslink density reaches its maximal value asymptotically. This is expected since as D_p is large enough at a fixed conversion, there is very little additional connectivity that can be gained in the network from eliminating the few "loose chain ends. For example, at high conversion levels, considering a D_p of 1000, which is increased sequentially by factors of 10 (for instance, as *q* is increased from 0.999 to 0.9999 to 0.99999 and so on, while *e* is set to 0), the additional number of effective crosslinks approaches 0 (as can be seen from the idealized model expressed in **Equation 2-11**) for each order of magnitude increase in D_p. As we go to lower conversions, as mentioned earlier, the absolute difference between the curves is diminishing so that at low conversions, the crosslink density converges even faster as *q* approaches unity.

Figure 2-5 demonstrates the effect of q on the curvature of the crosslink density as a function of conversion relationship. In the figure, the curve marked "0.92" was predicted for q=0.92 and was than multiplied by a constant factor so that its crosslink density at full conversion would equal to that the curve predicted for q=0.99. Since multiplying by a constant does not affect the second derivative of the curve, it is clear from the figure that as q decreases the curvature increases. This realization is important from a processing perspective, since often the conversion level fluctuates, and thus it is generally desirable to operate within a relatively constant crosslink density regime. This means that for applications where high conversion levels are desired, one would prefer a system with a high q value, while for low conversion applications a the low q system is desired. In this unrealistic example, the crosslink density for the low q system has been artificially increased by a constant factor. The next section which discusses the affects af on the crosslink density, suggests a physical way in which the crosslink density of a system can be substantially increased while minimizing the increase in curvature.

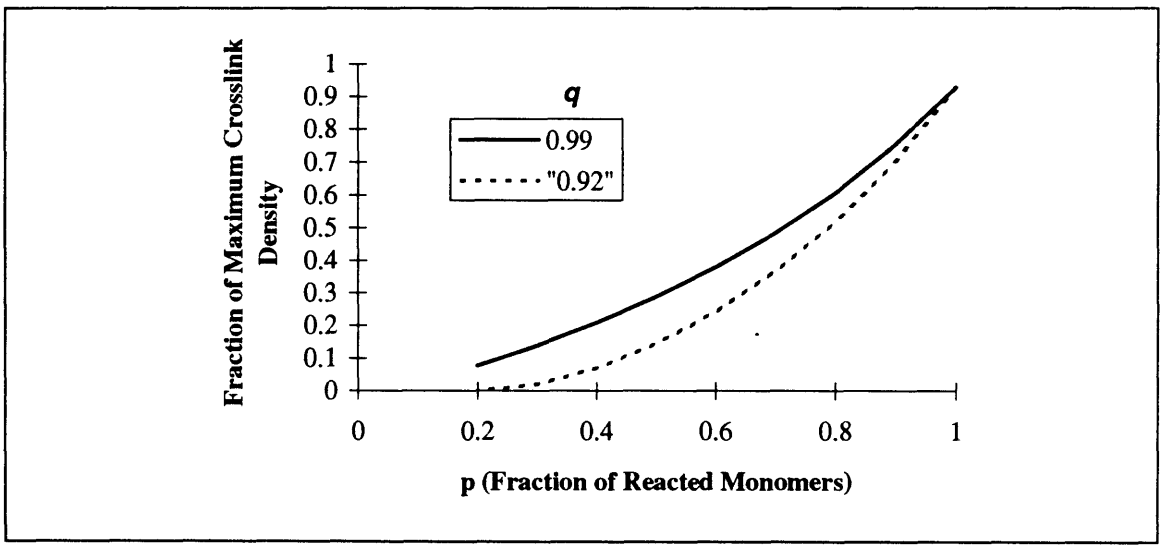

Figure 2-5. Comparison between two curves of predicted maximum crosslink density fraction as a function of conversion. The curve marked "0.92" was calculated for q=0.92 and than multiplied by a constant so that its full conversion crosslink density equals that of the curve calculated for q=0.99. For both curves, af=0.15 and e=0.5.

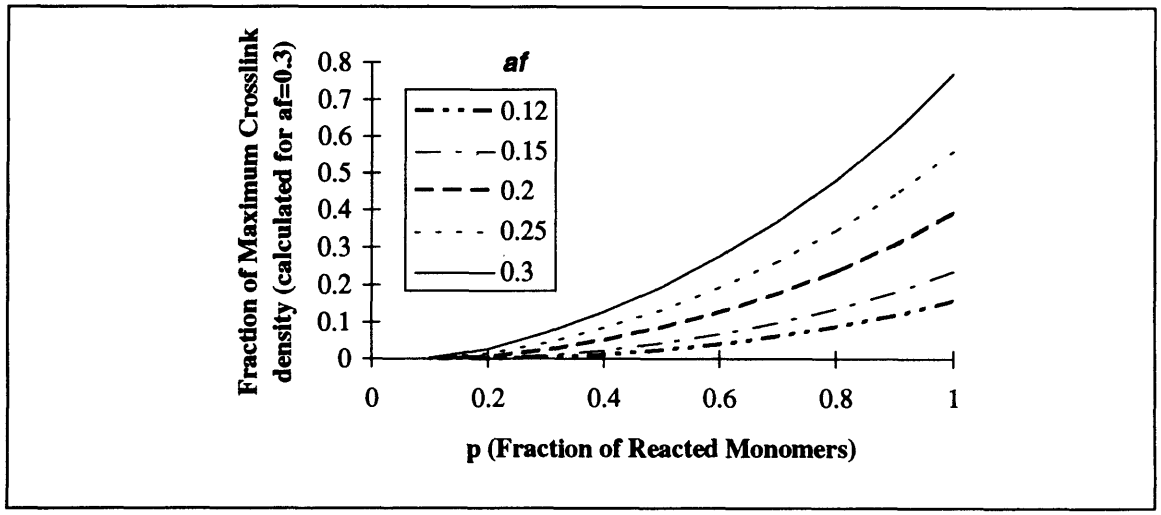

Figure 2-6. Predicted fraction of maximum crosslink density as a function of conversion for different *af* values. Calculations were made for q=0.95 and e=0.5.

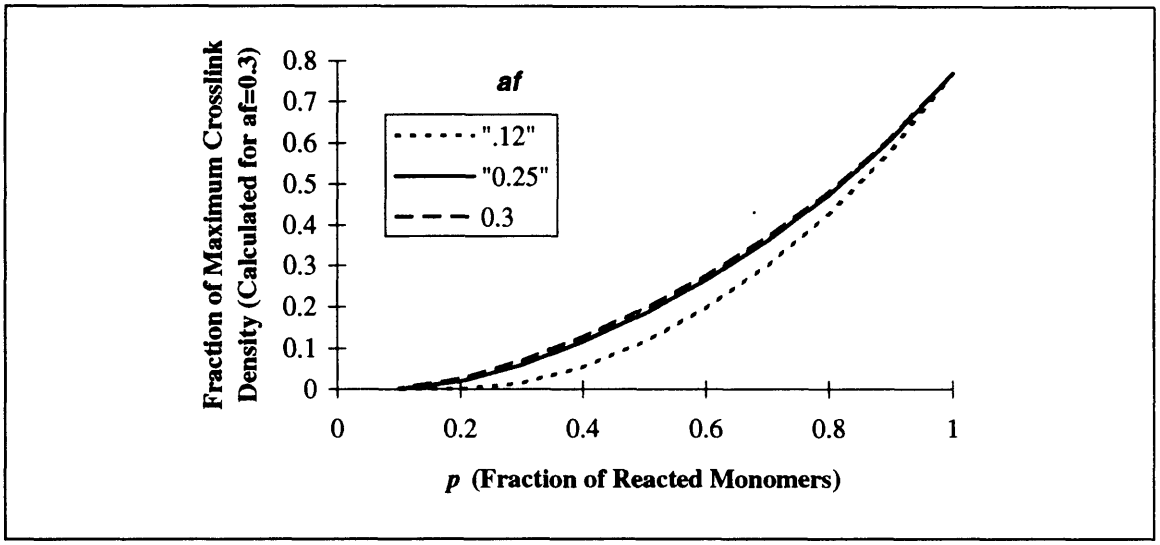

Figure 2-7. Comparison between two curves of predicted maximum crosslink density fraction as a function of conversion. The curves marked "0.12" and "0.25" were calculated for *af*=0.12 and 0.25, respectively. These curves were than multiplied by a constant so that their full conversion crosslink density equals that of the curve calculated for *af*=0.3. For all curves q=0.95 and e=0.5.

2.6.1.3 Appreciating the Influence of Parameter *af* on the Crosslink Density:

Figure 2-6 is analogous to **Figure 2-4** except that all curves of crosslink density as a function of conversion are generated by the model for the same q (=0.95) while each curve represents a different *af* value. The range of *af* values was chosen between 0.12 and 0.3 - the range of interest in this study. One should notice that for a given conversion level, unlike the case of varying q, the crosslink density diverges with increasing *af* (up to its maximum, unity). For q values approaching unity, the crosslink density is obviously expected to grow more linearly with increasing *af*. As shown in **Figure 2-7,** (analogous to **Figure 2-5**), the curvature of the crosslink density function increases with decreasing *af* values. Though qualitatively this trend is the same as earlier discussed for decreasing q values, one can readily notice that the influence of *af* on the curvature is significantly smaller than that of q. More will be discussed about this comparison in section **2.6.1.5**.

2.6.1.4 Appreciating the Influence of Parameter *p* on the Crosslink Density:

The importance of p as a parameter controlling the crosslink density for any system defined by its e, q, and *af* parameters has already been mentioned with respect to the positive curvature of the crosslink density as function of conversion. For example, looking at **Figure 2-6** one notices that for a typical system there is about a 30% increase in the crosslink density as a result of polymerizing the last 10% of residual monomers. Thus, leaving aside potential physio-chemical problems associated with controlling the level of residual monomer, the crosslink density at high conversions is often times extremely sensitive to the level of conversion. On the other hand, the positive curvature can be advantageous for controlling the crosslink density of low conversion applications in which the residual monomer presents no problem. Since in this particular study emphasis is put on high conversion levels, the positive curvature of the crosslink density function of conversion is seen as potentially problematic from a processing perspective. This point will be stressed later when discussing the characteristic kinetics of a free radical crosslinking polymerizations at high conversions.

2.6.1.5 Alternative Pathways to Consider When "Designing" the Network Structure

Having discussed the effects of e, q, p, and *af*, it can be concluded that for the common system in which one can ignore the importance of e, the crosslink density is dominated by q, p, and *af*. In most cases, of the three, *af* is the easiest parameter to manipulate since it

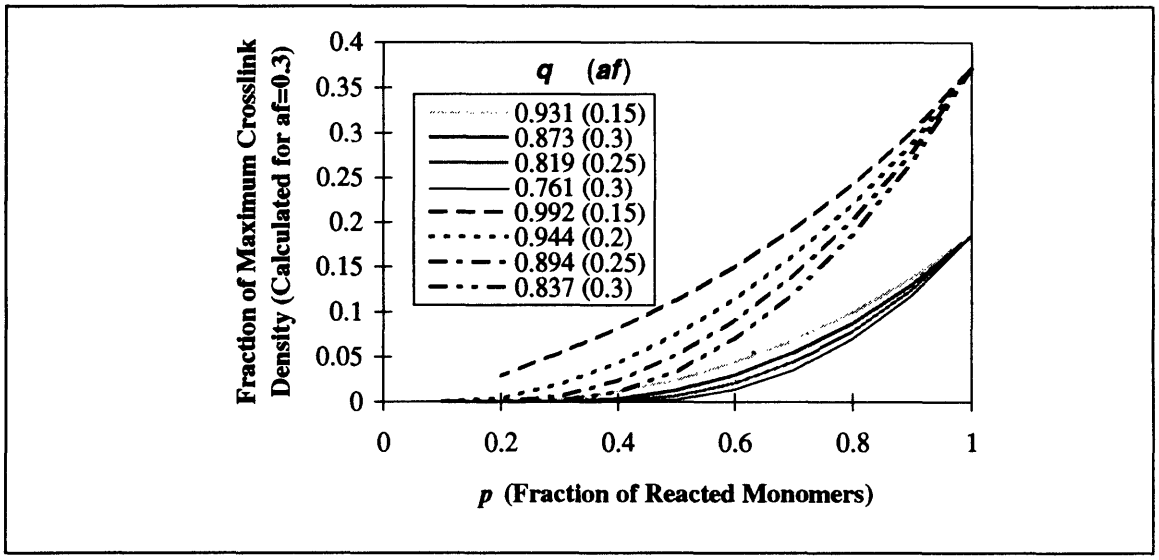

Figure 2-8. Fraction of maximum crosslink density (calculated relative to *af*=0.3 and for *e*=0.5) as a function of conversion, predicted for different combinations of *q* and *af* values with the constraint of equal crosslink density at full conversion.

Table 2-2

Comparison between the effects of *q* and *af* on the curvature of the crosslink density function for a given full conversion crosslink density (*e* = 0.5 in all calculations)

q	*af*	% difference in crosslink between full conversion ("100%" crosslink density) and 90% conversion
0.760676	0.3	36
0.814825		30
0.837489		28
0.930691	0.15	25
0.974267		21
0.99156		19

involves a simple change in the formulation by which the concentration of crosslinking components is altered. Controlling the conversion level in a low T_g photo-polymerized system such as the one discussed in this study, is reasonably easy as well, provided that one can reliably monitor the conversion level once the polymerization is stopped. For many applications, however, a minimal level of residual unreacted groups is desired, and thus, it is often not feasible to control the crosslink density by varying *p*. In light of this constraint which is generally imposed on this study, when designing the network structure, one should focus on changing *af* only, or, usually more challengingly, on manipulating *q* as well.

A quantitative perspective on the relative effects of *q* and *af* in a system shows that in order to achieve a given crosslink density at a given conversion, the statistical model suggests potential considerations involved in choosing a high-*q*-low-*af* system over a high-*af*-low-*q* system and vice versa.[xv] In other words, there are motivations to study ways of manipulating *q*, rather than simply rely on changes in the formulation to achieve desired network properties. In **Figure 2-8** the statistical model was used to compare crosslink density as a function of conversion curves between systems characterized by different combinations of *af* and *q* values with the constraint that at full conversion they generate the same crosslink density. In **Table 2-2** the percentage difference in crosslink density between full and 90% conversion is listed for the different systems. Clearly, the table indicates that *q* is the dominating parameter determining the crosslink density curvature with conversion. This curvature is practically independent of *af*, which further suggests that especially for applications in which close to full conversion is desired, a high-*q*-low-*af* system is preferable to a high-*af*-low-*q* system, both of which give the same crosslink density at full conversion.

[xv] Here we neglect the importance of *e*, however, more generally these considerations hold for choosing a high- D_p -low-*af* over a low- D_p-high-*af* system, while neglecting the *q/e* composition affect on the crosslink density for a given D_p.

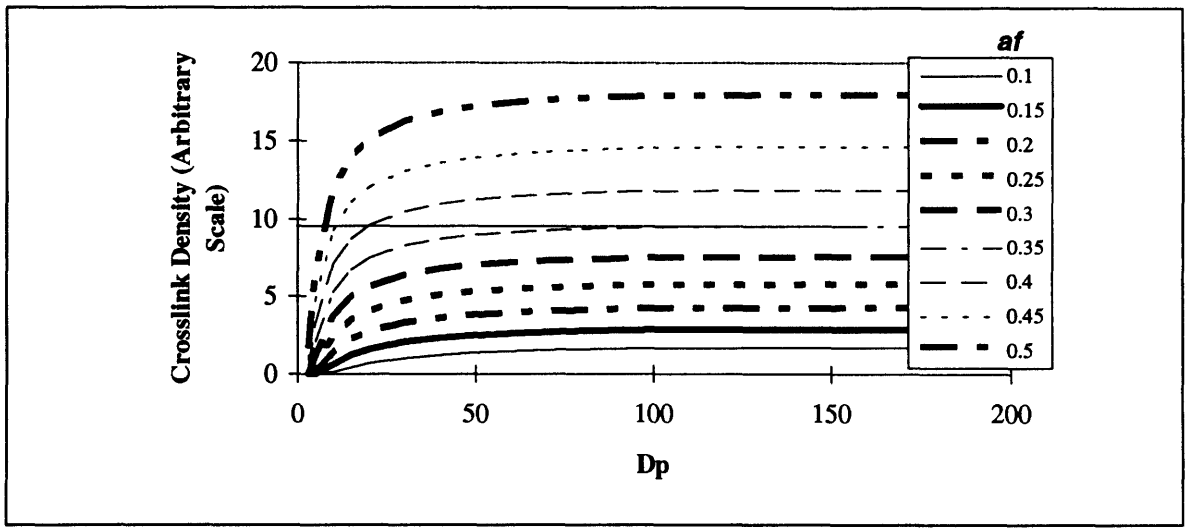

Figure 2-9. Full conversion crosslink density (arbitrary scale) as a function of D_p (e=0) for a series of different af values as predicted by the statistical model.

Another advantage in using a high-q-low-af system rather than a low-q-high-af system to achieve a specified crosslink density at any fixed conversion level is demonstrated in **Figure 2-9**, which gives the crosslink density (at full conversion in this case) as a function of D_p (which in the usual case correlates mainly with q, while the effects of e can be neglected) for a series of af values. For example, if one aims at a full conversion crosslink density of 9.5 (arbitrary scale) as indicated by the horizontal line, one is faced with the options of choosing systems having any af values between 0.35 and 1. The corresponding D_p value would be determined from the intersection point between the horizontal line and the curve corresponding to the chosen af value. When considering expected fluctuation in D_p due to changes in the free radical kinetics (as a result of polymerization temperature changes, impurities acting as transfer agents, etc.) one realizes that the curve corresponding to the smallest af value sufficient to achieve the desired crosslink density is the optimal choice. That is the case, since such a system would require a high D_p value to achieve the desired crosslink density so that one would operate in the flat region of the curve, where the crosslink density is most robust to expected D_p fluctuations. In the example above, it would be optimal to choose a system having af=0.35 and D_p>100 (the larger D_p, the better.)

2.6.2 Incorporating the Temperature and R_i Effects on the Free Radical Kinetics into the Statistical Network Model

In essence, the approach for introducing the temperature and initiation rate effects on the resulting network structure would be to simply plug the T and R_i dependent step rate expressions derived earlier into the model parameters q and e. The model would then in theory predict crosslink density and other structural descriptions as a direct function of T, R_i, af, and p. The problem with this procedure is that the resulting equations to be solved by the model become far more complicated, and one looses an intuitive grasp of the T and R_i effects from the expressions themselves. Therefore, having already established the basic relationships between e, q and the predicted crosslink density while taking into account the influence of af and p, we need to focus on the direct influences of T and R_i, on q and e (naturally, af and p are independent of T and R_i here).

By combining **Equations 2-2** through **2-4** with the expressions for e and q, and substituting Arrhenius expressions for the respective rate constants, we get **Equations 2-12** and **2-13** which give e and q respectively as functions of T, R_i and p.

$$\frac{1}{e} = 1 + \frac{A_{td}}{A_{tc}} e^{\frac{-(E_{td}-E_{tc})}{RT}} + \frac{\sqrt{2}}{A_{tc}R_i^{1/2}} \sum \left(A_{trx}[X] \left(A_{td} e^{\frac{-(2E_{trx}+2E_{tc}-E_{td})}{RT}} + A_{tc} e^{\frac{-(2E_{trx}-E_{tc})}{RT}} \right)^{1/2} \right) \quad \textbf{(2-12)}$$

$$\frac{1}{q} = 1 + \sum \left(\frac{A_{trx}[X]}{A_p(1-p)[M]_0} e^{\frac{-(E_{trx}-E_p)}{RT}} \right) + \frac{\sqrt{2}R_i^{1/2}}{A_p(1-p)[M]_0} \left(A_{td} e^{\frac{-(E_{td}-2E_p)}{RT}} + A_{tc} e^{\frac{-(E_{tc}-2E_p)}{RT}} \right)^{1/2} \quad \textbf{(2-13)}$$

For a given temperature and conversion level, increasing the rate of initiation would result in increasing e (for $R_{tc}>0$) while decreasing q. These two results would in theory tend to have opposing effects on the crosslink density. In practice, however, the case in which increasing R_i would increase the crosslink density is merely a mathematical curiosity which corresponds to the previously discussed case of increasing D_p with R_i for linear systems. For systems and temperature ranges in which transfer and/or combination rates can be neglected relative to R_i, e would be independent of R_i as the third term of **Equation 2-12** would diminish relative to the other terms. In these cases, it is easy to see that any increase in the rate of initiation would strictly reduce the crosslink density.

Assuming for the sake of argument that q is independent of R_i, for cases in which $R_{tr}/R_i >> 1$, e would be restricted to values close to 0, and thus, no significant effect on the crosslink density would be observed as a function of R_i For cases in which R_{tc} approaches R_i (combination is the dominating termination mechanism), R_i can theoretically determine e to be anywhere between 0 and 1, however, such variations will change the crosslink density significantly only under conditions in which q is small enough as discussed in Section 2.5.1.1. Since in reality q decreases with R_i, and since one can usually neglect the importance of e relative to that of q in controlling the crosslink density, the key to quantitatively control the crosslink density by changing R_i, is to understand q as a function of the initiation rate.

For $R_{tr} >> R_i$, if q is close to 1 (that is $R_p >> R_{tr}$) changes in R_i will have little effect on q and even less on the crosslink density since at high q values, the crosslink density approaches asymptotically its maximum value for any given conversion level. When $R_{tr} >> R_i$ but transfer is not negligible relative to propagation, changes in q with R_i will be small, however, these changes may have significant effects on the crosslink density, since we are in a small q regime where the crosslink density is sensitive to q. For $R_i >> R_{tr}$, if $R_p >> R_i$, q is close to unity and relatively constant with R_i so that the crosslink is not affected by R_i. When $R_i >> R_{tr}$ but initiation is not negligible relative to propagation, q is less than unity and varies significantly with R_i so that the crosslink density is a strong function of the initiation rate at any conversion level.

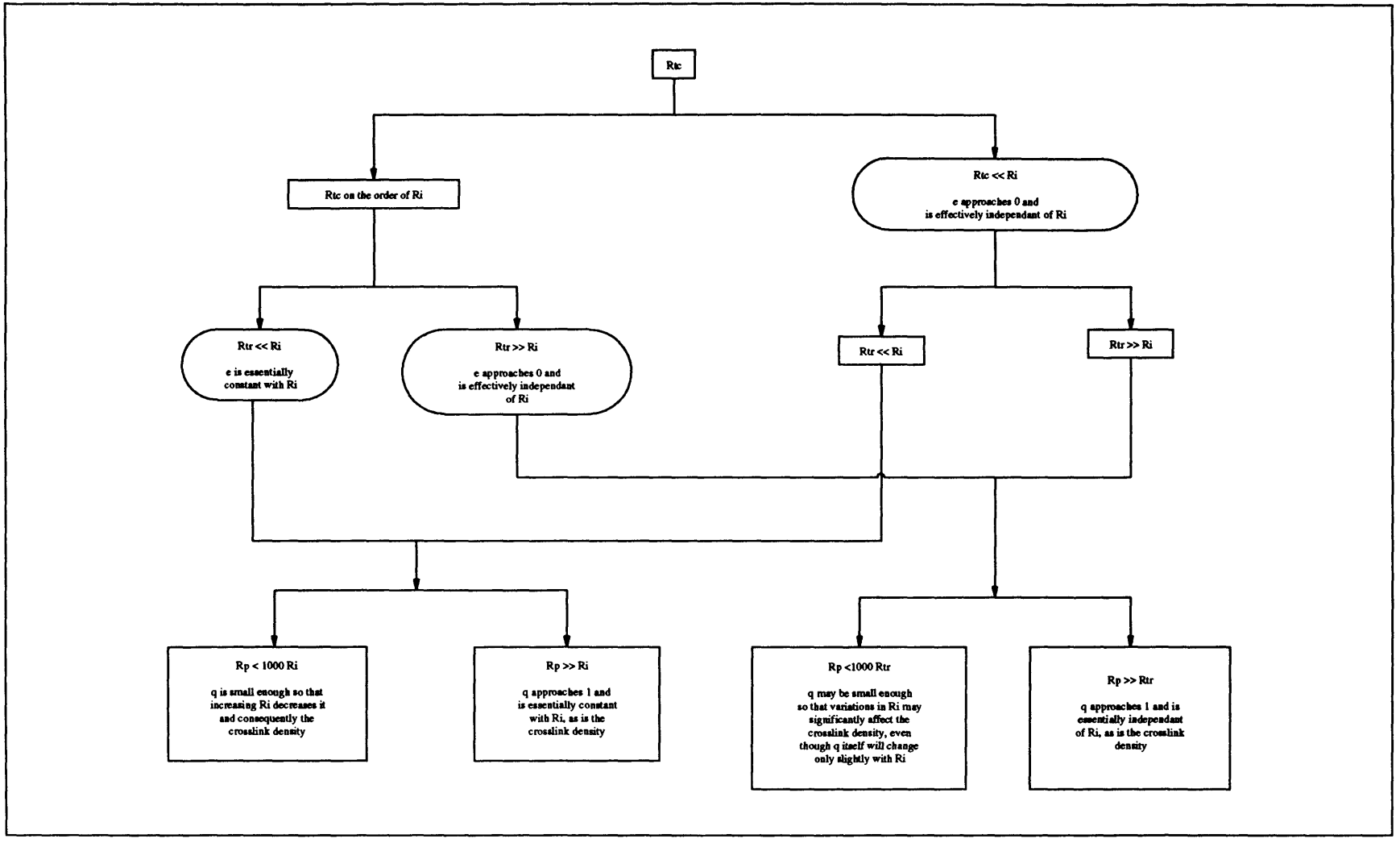

Figure 2-10. Flow chart showing the expected effect on the crosslink density as a result of changing the initiation rate.

Figure 2-10 summarizes the important expected effects of R_i on the crosslink density via parameters *e* and *q* as based on the statistical model. Based on the analysis it can be stated that for all practical purposes, the crosslink density of a system at a fixed temperature and conversion, would decrease with increasing rate of initiation. Also, for all practical purposes, when using the model to study the quantitative effects of R_i on the crosslink density we can ignore *e* and focus only on changes in *q*.

As for the effects of changing the temperature, one should not be surprised that qualitatively the inequality conditions derived for increasing D_p are in complete agreement with the conditions for increasing *e* and *q* in the non linear case. Again, this finding is expected, considering that for a given conversion level, the crosslink density increases with both *e* and *q* while the relation between D_p and the crosslink density has already been demonstrated. More quantitatively, one can use an analysis similar to the one presented in **Figure 2-10** to get an idea of the conditions under which changes in the magnitudes of the rate constants with temperature would generate significant changes in the expected crosslink density. As was discussed in section 2.5.1.1, a shift (with polymerization temperature in this case) from one termination mechanism to another would significantly affect the crosslink density only if transfer can be neglected relative to the initiation rate, and the initiation rate cannot be neglected relative to the propagation rate. These conditions rarely embody a realistic case which is advantageous since generally one can then attribute changes in the crosslink density with polymerization temperature to changes in *q* rather than a combination of *q* and *e*.

In summary, considering both R_i and polymerization temperature effects on the crosslink density, one can generally ignore changes in parameter *e* as a dominating factor controlling the crosslink density. Experimenting in an "*e* independent" regime is convenient considering the difficulties involved in monitoring the termination mechanism as a function of temperature. In the analysis of results, one can therefore generally eliminate *e* as one degree of freedom, and focus instead on direct changes in parameter *q* to explain changes in crosslink density with initiation rate (or, irradiation intensity here) and polymerization temperature.

Section 3: Experimental Procedure

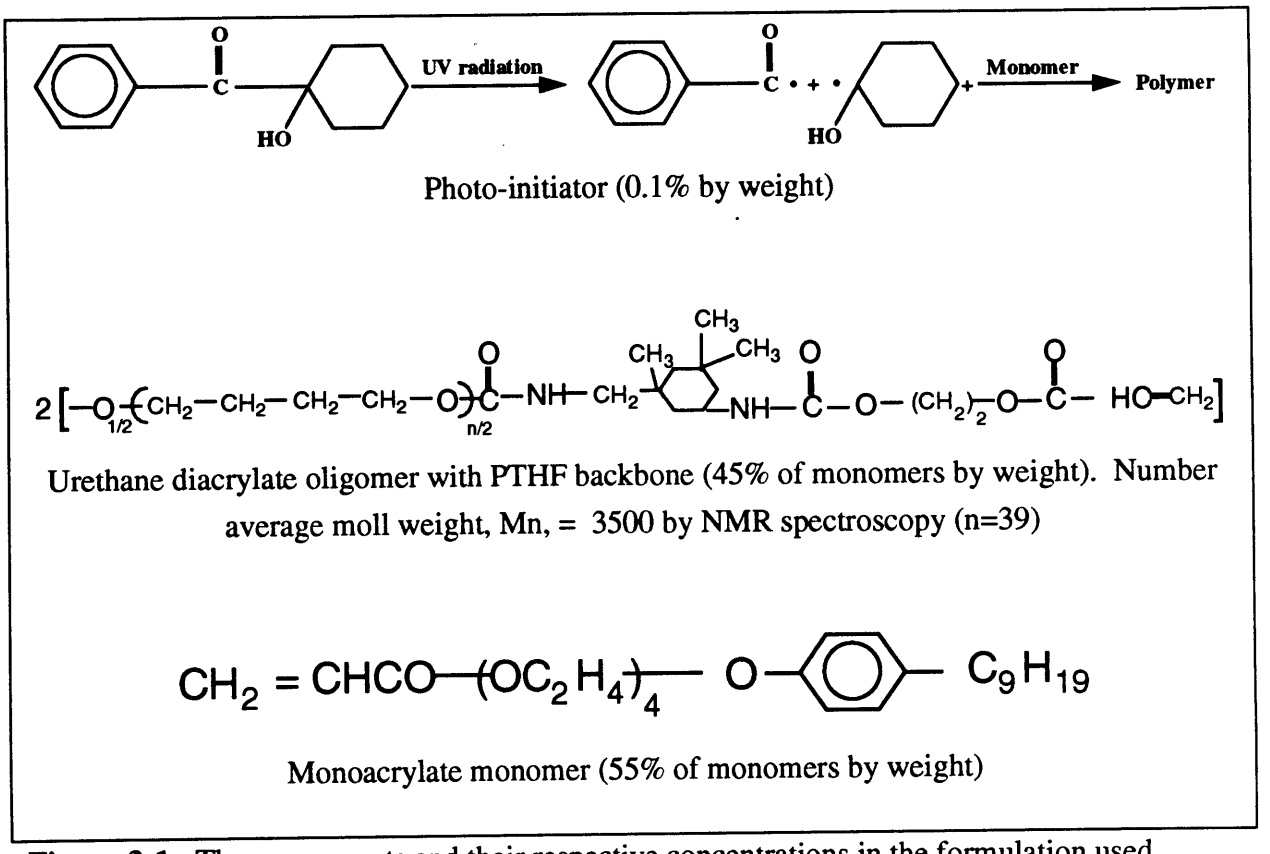

Figure 3-1. The components and their respective concentrations in the formulation used as the study model system for experimentally investigating effects of photo-polymerization temperature, initiation rate, and conversion on network structure formation.

3.1 Choosing the Model System

Figure 3-1 shows the composition of the chosen model system for this study, including the monofunctional and difunctional monomers (the latter of which is by itself an oligomer), and the photo-initiator. Though in principle statistical models can be employed for studying network structures of any multi-component free radical system under the assumptions discussed, there are a number of considerations that have been taken into account while choosing the particular system of this study. From the model's perspective, the more complex the system, the more cumbersome and the less intuitive the derived expressions, and thus, the harder it is to quantitatively analyze empirical data by conclusively fitting results to model predictions. Most important in this experimental study are the experimental limitations imposed on our attempt to actually monitor the structural development of the polymerizing network under varying conditions of temperature and initiation rate.

The basic guideline, therefore, for choosing the free radical network forming model system was to keep it is as simple as possible while attempting to satisfy model assumptions over the experimented range of temperatures and initiation rates. Not less important was satisfying assumptions involved in the macroscopic measurements of properties which serve as indicators of the underlying network structure. Listed below are some requirements for satisfying the various assumptions, along with the respective desired physico-chemical and structural characteristics of the system's components and its polymerized network.

Statistical model and steady state free radical assumptions. The abssence of rate limiting radical mobility throughout the polymerization raction is important for satisfying the free radical steady state assumption according to which termination is not diffusion controlled as function of the conversion level. An implicit condition for this to happen is that the system's polymeriation temperature is sufficiently above the T_g of the fully cured network. The system of choice should therefore have a low enough T_g to enable a wide range of polymerization temperatures to be experimented under this assumption. It should be mentioned that diffusion controlled termination, often also referred to as Thromsdorf effect, is generally associated with bulk polymerizations. This should raise a relevant concern considering the absence of any solvent in the experimental system used here. Nevertheless, to the best of our knowledge, the published data indicating the presence of

Thromsdorf effect has consistently described systems polymerized below or close to the T_g of the polymer, suggesting that bulk polymerization by itself may not be a sufficient condition for diffusion limited termination kinetics.

To satisfy the equal reactivity assumption of all identical functional groups, naturally the two components need to have the same chemical functional group, acrylates in our case. It is also required that the two components be completely miscible in one another at the concentration and temperatures explored, forming no micro-phase separations, (the oligomer component is thus assumed to occupy the random flight conformation before as well as after polymerizing).

To satisfy the independence of reactivity assumption between the two reactive groups of the difunctional species, an oligomer was chosen as the crosslinking component. The relatively large distance between the two acrylate groups of the difunctional oligomer is expected to minimize strenic and iductive effects, thus eliminating the interaction between them so that as the first reacts, the other's mobility would be essentially unaffected, making its reactivity independent of its partner's.

"Processing" considerations. To assure a uniform network structure across the thickness of a photopolymerized film, the photoinitiator absorption needs to be low enough. This can be achieved by making the film thinner, irradiating simultaneously from both sides, lowering the concentration of photoinitiator, and/or irradiating at the low absorptivity portion of the photo-initiator's absorption spectrum. The last mentioned option is especially useful when taking into account the constant initiation rate assumption which requires a high enough initiator concentration so that the polymerization reaction consumes only a negligible fraction of the starting amount for a given irradiation intensity and conversion level. Since making very thin films would have a negative effect on modulus measurements accuracy, this option is least preferable for our purposes. Using a reflective surface underneath the film is one way to create a double sided irradiation mechanism which would minimize non uniformities. Such a setup is usually unnecessary if the absorbence can be maintained as low as 0.05 which would result in less than ten percent difference in initiation rate between opposing sides of the film. As earlier mentioned, the photo initiator is also assumed to dissociate sufficiently independent of the polymerization temperatures explored, and the two radicals thus formed, are assumed sufficiently equally reactive at temperatures.

In order to control the temperature throughout the exothermic polymerization reaction, a low enough polymerization rate is required. This requirement is partially satisfied by the law concentration of initiator. Another advantage of having a relatively slow polymerization rate is that one can more accurately monitor the kinetics and control the samples level of conversion.

In order to achieve dimensional stability of the thin liquid films when polymerized at relatively high temperatures, a relatively high viscosity was desirable. The components chosen, therefore, are of high enough molecular weights. High molecular weights are also important for minimizing evaporation of some components during high temperature curing.

Macroscopic network properties. In order to approximate the behavior of a perfect elastomer, the network should have a low enough crosslink density, and minimal enthalpy-driven molecular interactions in the cured and partially cured states (see Section 3.4.1). These requirements are satisfied by use of a sufficiently low concentration of crosslinking components, and choosing monomers having no inter or intramolecular hydrogen bonding. A simple free radical polymerized entropy network of this kind would in this case be a two component system composed of a high molar concentration of mono functional relative to difunctional monomer.

3.2 Preparing the Monomer Solution

The photoinitiator was provided by CIBA-GEIGY (under the commercial name Irgacure® 184). The monofunctional monomer, ethoxylated nonyl phenyl acrylate, and the difunctional monomer, an alyphatic polyether urethane diacrylate oligomer, were both availabe from commercial sources. No further purifications were performed on any of the components. The solution consisting of the concentrations given in **Figure 3-1** was prepared by mixing the components for about 5 hours at slightly elevated temperatures (<50°C) to increase mixing rate without inducing spontaneous polymerization or evaporations.

3.3 Characterizing the System

Having chosen the model system, several characterization techniques were employed to verify presence of some of the desired properties for satisfying the assumptions as

discussed in Section 3.1. IR and quantitative C NMR spectroscopy were used to determine the chemical composition of the diacrylate oligomer backbone, and detect the presence and concentrations of impurities. Analysis of NMR results was used to calculate Mn of the diacrylate oligomer. Thermogravimetric analysis was used to assess the high temperature resistance of the system to evaporation of low molecular weight components. DSC analysis[30] was used to determine T_g of the uncured system as well as the fully cured network. UV Spectroscopy was used to determine the spectral absorbence of the photoinitiator, and the background absorbence due to the monomers. The absorbance of the initiator is important for determining the initiation rate for a given irradiation spectra and intensity, (through parameter K from **Equation 2-1**). The background absorbance is important for calculating the overall absorbance in order to determine the uniformity of the initiation rate and thus uniformity of the network structure across the thickness of the film.

3.4 The Scheme for Generating the Data

In this study we are primarily interested in experimentally evaluating the effects of the three "processing controlled" variables, T, p, and R_i, on the structural development of the network, and specifically, on the network crosslink density which is the central dependent variable. Macroscopically, the network structure is investigated by measuring equilibrium tensile modulus and T_g as two structure determined properties. The experimental procedure can therefore be outlined in four basic steps described in Sections 3.4.3 through 3.4.6. The following sections discuss the theory underlying the qualitative and quantitative application of the macroscopic properties as measured to determining the crosslink density of the network.

3.4.1 Using Equilibrium Tensile Modulus as a Macroscopic Gauge of the Crosslink Density

3.4.1.1 General

An ideal entropy elsatomer is modeled as a collection of individual entropy springs assembled in a parallel configuration. The modulus of such a system is calculated form the total sum of contributions made by each polymer segment serving as an effective entropy spring. To be an effective entropy spring a polymer segment has to: 1) extend to the infinite network from both directions 2) be long enough so that the random flight configuration would be applicable for calculating the entropic driving force resisting

applied strain. 3) have negligible inter and intramolecular enthalpic interactions when considering the total free energy changes associated with stretching the network. Naturally, this requires that the polymer network be above T_g to be considered an entropy elastomer.

By calculating the entropic free energy penalty associated with applying an affine tensile deformation to a system satisfying the above conditions and acting under thermodynamic equilibrium at constant pressure, one gets the relationship expressed in **Equation 3-1.**[17]

$$E = RT[C]\left(\alpha + \frac{2}{\alpha}\right) \cong 3RT[C] \qquad \textbf{(3-1)}$$

Where E is the equilibrium tensile modulus, R is the gas constant, α is the ratio between the length of the strained and relaxed sample, and [C] is the molar concentration of effective entropy springs. The RHS approximations is valid for small strains in which case α approaches 1.

It should be noted that empirical data showing T and [C] dependence of the modulus have generally been in good agreement with theoretical predictions for small deformations. More complicated theories have been proposed to explain deviations from these predictions at larger deformations, and to account for such effects as of non-affine deformation, permanent entanglements, strain induced crystallization, and non-equal contribution to stress between chains connected to crosslink points of different functionalities. Since there is no substantial evidence to suggest that for our purposes the more complicated models give better predictions (especially not having the data for some of their required parameters), in this study, the interpretation of equilibrium tensile modulus data relies on the ideal elastomer assumption behaving under small strains as expressed by **Equation 3-1.**

3.4.1.2 Applying the Theory of Elasticity to the Study Model System

Assuming that under appropriate conditions the system employed in this study can be successfully approximated as an ideal elastomer (see Section 3.1), we can establish a

relationship between the effective density of entropy springs and the effective crosslink density predicted by the statistical model. Once we have found the crosslink density, we can back calculate q for a given af and conversion level (assuming e can be ignored).

In Section 2.5, when discussing **Figure 2-2** it was shown that the difunctional unit can have either 1,2,3 or 4 arms extending to the infinite network while the difunctional has only 1 or 2. Fur purposes of counting effective density of entropy springs, we need only consider difunctional units with 3 or 4 infinite arms. However, while earlier when discussing the general case, we considered a 4-infinite-arms unit as representing one 4-point-crosslinker, here we consider it as two 3-point-crosslinkers. The reason for this, as can be seen in **Figure 2-2**, is that the backbone of the oligomer diacrylate unit used here is sufficiently long to be considered an entropy spring by itself. Therefore, the difunctional unit can serve as either one or two 3-point-crollinkers depending on whether it has 3 or 4 arms extending to the infinite network, respectively. **Equation 3-2** establishes this relationship.

$$\begin{pmatrix}\text{effective}\\ 3-\text{point}-\text{crosslink}\\ \text{density}\end{pmatrix}=\begin{pmatrix}\text{model predicted}\\ 3-\text{point}-\text{crosslink}\\ \text{density}\end{pmatrix}+2\begin{pmatrix}\text{model predicted}\\ 4-\text{point}-\text{crosslink}\\ \text{density}\end{pmatrix} \tag{3-2}$$

Since each 3-point-crosslink is connected to 3 entropy springs, and each spring is shared between 2 3-point-crosslinks, in order to get the 3-point-crosslink density we need to multiply the entropy spring density by a factor of 2/3. So, combining **Equation 3-1** with **Equation 3-2** and the above stated relationship, one gets a linear expression for the 3-point-crosslink density of the network as a function of the equilibrium tensile modulus:

$$\text{effective } 3-\text{point}-\text{crosslink density} \cong \frac{2}{9RT}E \tag{3-3}$$

3.4.2 Using T_g as Macroscopic Gauge of the Crosslink Density

In general, correlations between T_g and the crosslink density of the network are more complicated than the simple relationship between a crosslink density and the equilibrium tensile modulus for an ideal entropy elastomer as expressed by **Equation 3-3**. For a relatively loosely crosslinked network such as in this study, a high sensitivity of the T_g measurement is required to observe differences in the crosslink density between two networks of the same composition and degree of conversion. In theory, however, the increase in the crosslink density should correlate, at least qualitatively, with an increase in

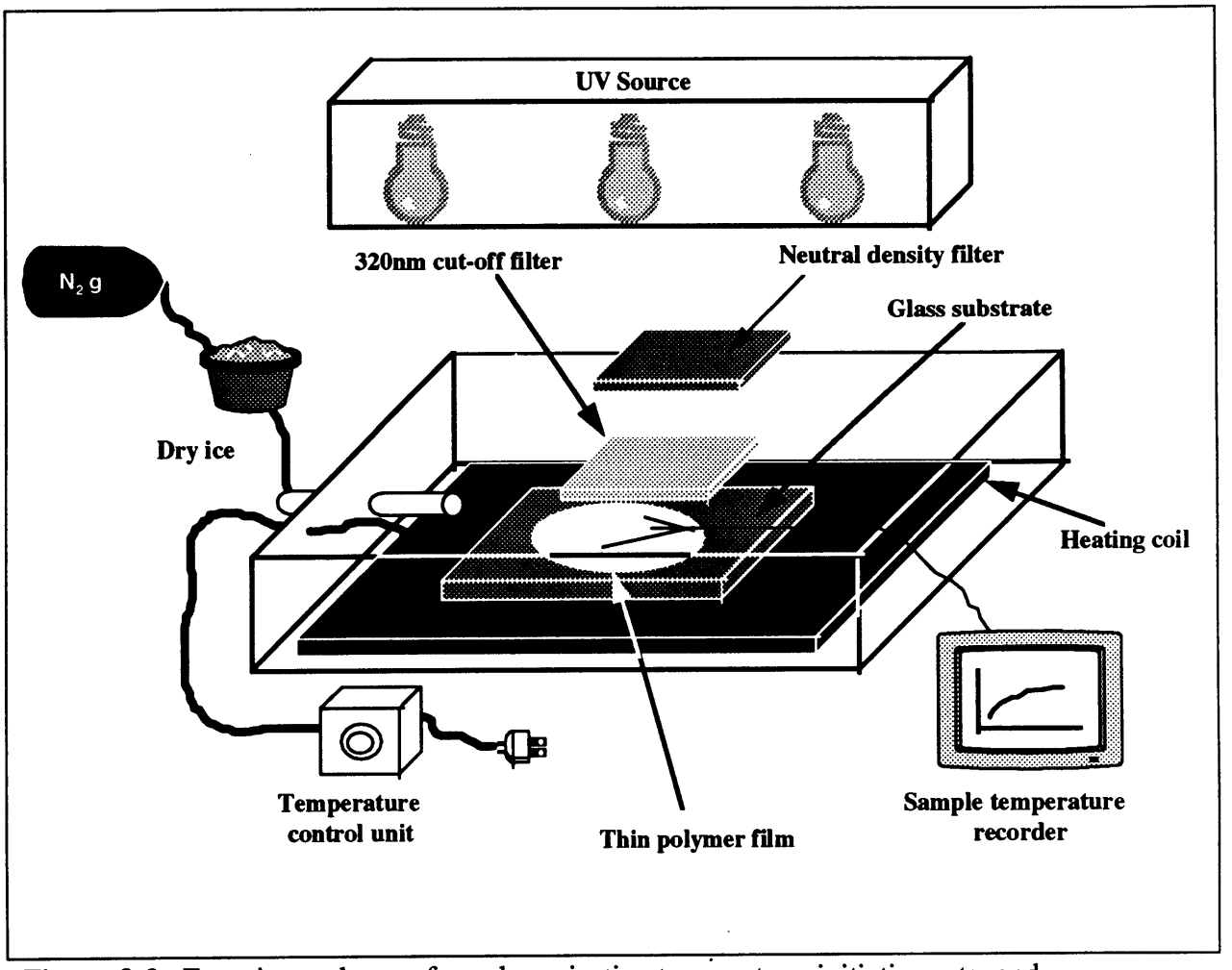

Figure 3-2. Experimental setup for polymerization temperature, initiation rate, and conversion controlled photo-polymerization of thin films.

T_g.[31] In this study, T_g measurements were done quantitatively as a function of conversion only, and mainly in order to characterize the system and find a possible correlation between the increase in T_g with conversion and changes in kinetics as a function of conversion and polymerization temperature.

3.4.3 Controlling the Photo-polymerization Process

Figure 3-2 shows a schematic of the experimental setup for curing thin films to varying degrees of conversion and under controlled conditions of polymerization temperature and initiation rate. Films are made by drawing a 1 gram sample of monomer solution onto a glass substrate. The average thickness of the films was 0.03 cm. Films were irradiated on the glass substrate and, throughout the curing process, were subject to a nitrogen atmosphere maintained by a steady $N_{2(g)}$ flow over the sample and through the UV-transparent irradiation chamber which allowed for the gas to escape. Prior to irradiation, films were left to equilibrate with the nitrogen atmosphere for five minutes in order to assure removal of most dissolved oxygen from the monomer solution.

The polymerization temperature was controlled by a heating plate connected to the temperate control unit. On top of this unit lies the glass substrate with the film facing upward towards the UV lamp. Using thermo couples directly embedded in the film, a recording device recorded the film temperature as a function of time, both during steady state prior to irradiation, and during the polymerization reaction as the temperature increases due to exothermic polymerization heat. Increasing the rate of nitrogen flow and cooling it down with dry ice, can reduce the exothermic increase in temperature through improved convection. It is also possible to further stabilize the temperature during polymerization by using a better heat conducting substrate than the glass plate used. A metal would be one possibility.

Since generally the photo-intiator concentration is kept fixed in the formulation, the initiation rate was controlled by changing the irradiation intensity which is proportional to R_i as shown in **Equation 1**. The UV source used was a "Spectroline® EN-160L" lamp which has a maximum intensity of about 3 mW/cm^2, and a spectral output as shown in **Appendix A** which also oultlines the procedure used for estimating R_i. Films to be irradiated are positioned relative to the UV source so that a marked area is uniformly irradiated within <5% of the average intensity. The irradiation intensity can be reduced both by increasing the distance between the source and the film and/or by inserting neutral density filters between the source and the film.

The degree of conversion, p, is controlled by adjusting the films' irradiation exposure-time so that the photo-polymerization reaction can be stopped at any point between the starting point (0% conversion, or, $p = 0$) and the time required for full conversion (<1% residual monomer, or, $p > 0.99$). The time scale for full conversion of the typical film in this system is on the order of one to ten minutes. The starting and ending points of irradiation are controlled manually by opening a shutter at time 0 to begin exposure, and turning off the source at the end of exposure. This manual procedure does not affect the accuracy of the film's conversion level which is measured directly by NIR spectroscopy (see next section), however, it is not ideal for generating kinetic curves, especially at the lower conversion levels where short exposure intervals are required.

3.4.4 Measuring Conversion

Transmission NIR spectroscopy was used to determine the conversion (p) of each film.[4,34] Films were mounted while sitting on the (NIR transparent) glass substrate on which they were originally cured. The residual acrylates were indicated by the difference between two spectra, the first obtained shortly after the original UV irradiation, and the second taken after an additional intense dose was applied to assure full cure of all residual unreacted acrylate groups in the original sample. This difference spectrum, which shows distinct peaks due to the residual acrylates (in the 4400-6400 cm^{-1} region) is calibrated against the difference spectrum between the fully uncured ([M] = $[M]_0$,or p=0) and fully cured ([M] = 0 or p=1) states of a sample of known thickness. The calibration procedure is done by a computer program which uses the second derivatives of the spectra and normalizes for thickness variations between samples. The NIR technique for measuring p gives a resolution of about 1% conversion with decreasing accuracy as the residual acrylate concentration falls below 10-5%. **Appendix B** shows a typical NIR difference and cured spectra along with the associated computer program outputs. For more details on this procedure, see Refs. 3 and 34.

3.4.5 Equilibrium Tensile Modulus Measurements

Equilibrium tensile modulus was measured for all films of high enough conversion so that test sample preparation and measurement were possible with the instruments and procedure used. Test samples were prepared by cutting a 0.5cm wide and 2-5cm long strips from the irradiated films. The thickness variations within each test sample ranged usually within 5-10% of the average thickness. Equilibrium tensile modulus was measured at room temperature using a Rhevibron (model RHEO-200). This instrument allows for

manual strain adjustment and stress readings. Modulus was calculated from 7-10 stress-strain points with strain levels less than 4%.

Modulus results were reproducible within 1-3% for strips taken from the different films cured under identical conditions with relatively high conversions. For these films, modulus measurements, the greatest source of error results from high fluctuations in film thickness which is the usual case for films cured at higher temperatures. These films require use of a relatively short strip as a test sample, and as a result, the standard error for modulus determination often increases causing reproducibility to decrease with increasing temperatures of cure. For relatively low conversion films (<50%), reproducibility decreases as the error may increase up to 15% of the average value of these low modulus samples. The increase in the % error for low cure films is explained by the sensitivity of the instrument to absolute differences in stress, so that the smaller absolute differences in stress with increasing strain represent a higher percentage error in the low modulus films relative to the high cure, high modulus films.

3.4.6 T_g Measurements

Test samples of about 10 mg were prepared from irradiated films. T_g was measured in a PERKIN-ELMER 7 Series Thermal Analysis System operating at 15°C/min. The onset and end of the glass transition, the T_g point (defined here as the temperature at which C_p reaches the mid-point value between the glassy and rubbery states) and ΔC_p, were determined by use of the software provided with the instrument in combination with manual adjustments when necessary.

3.4.7 Predicting the Modulus and Calculating *q*, *e*, and/or *af* by Fitting Modulus and Conversion Data to Model Predictions

Model predictions were made by use of a spreadsheet program, (Microsoft Excel 4.0), which took into account the individual free radical rate parameters (with their built-in temperature and initiation rate dependence), composition, and conversion to calculate the crosslink density as a function of polymerization temperature and initiation rate, or directly as functions of *q* and *e*. Predictions of crosslink density as a function of *af* and *p* were made in the same manner. Similarly, a program was also used to back calculate *q* and *e* values for a given modulus, conversion, and *af* values. Conversely, one could calculate *af* given conversion, *q*, and *e*. The different programs also allowed for simultaneous fits between the kinetic data and the modulus data as functions of polymerization temperature

and initiation rate by predicting appropriate activation energies and prefactors for the different Arrhenius rate constants.

Section 4: Results and Discussion

4.1 Characterization Results

4.1.1 Monofunctional Monomer

Photo-polymerization of the monoacrylate by itself indicated that it formed permanent crosslinks even at conversions below 40%. In order to quantify the extent of this finding, equilibrium tensile modulus was measured for a fully cured film of the monoacrylate. The modulus determined represented only 10-15% of the modulus of the fully cured mono/diacrylate model system when polymerized under identical conditions. Since the intrinsic contribution of monoacrylate crosslinking was small but not negligible, two mechanisms were proposed to explain this result:

- Transfer to the monoacrylate, particularly to the CH_2 closest to the benzene. Such transfer would cause branching which could lead to permanent crosslinking at high enough conversions provided that there is sufficient termination by combination.

- The presence of crosslinking impurities within the mono-acrylate. Considering the fact that we are using a commercial product, and considering the steps used in synthesizing the monomer, it is very likely that impurities in the form of diacrylates are present.

It was also found, that the equilibrium tensile modulus of the polymerized, monofunctional monomer drops with increasing polymerization temperature for a given conversion. This further suggests mechanism 2 as the real explanation for the mono-acrylate intrinsic crosslinking since, if mechanism 1 were true, one would expect an increase in transfer to the monomer (and therefore an increase in the crosslink density and modulus) with increasing polymerization temperature which is not the case. The concentration of the assumed diacrylate impurity can be calculated from the modulus data and using the model given q (and neglecting the importance of e). Once the crosslinker concentration is determined, one can add it to that of the oligomer diacrylate to improve the fitting of

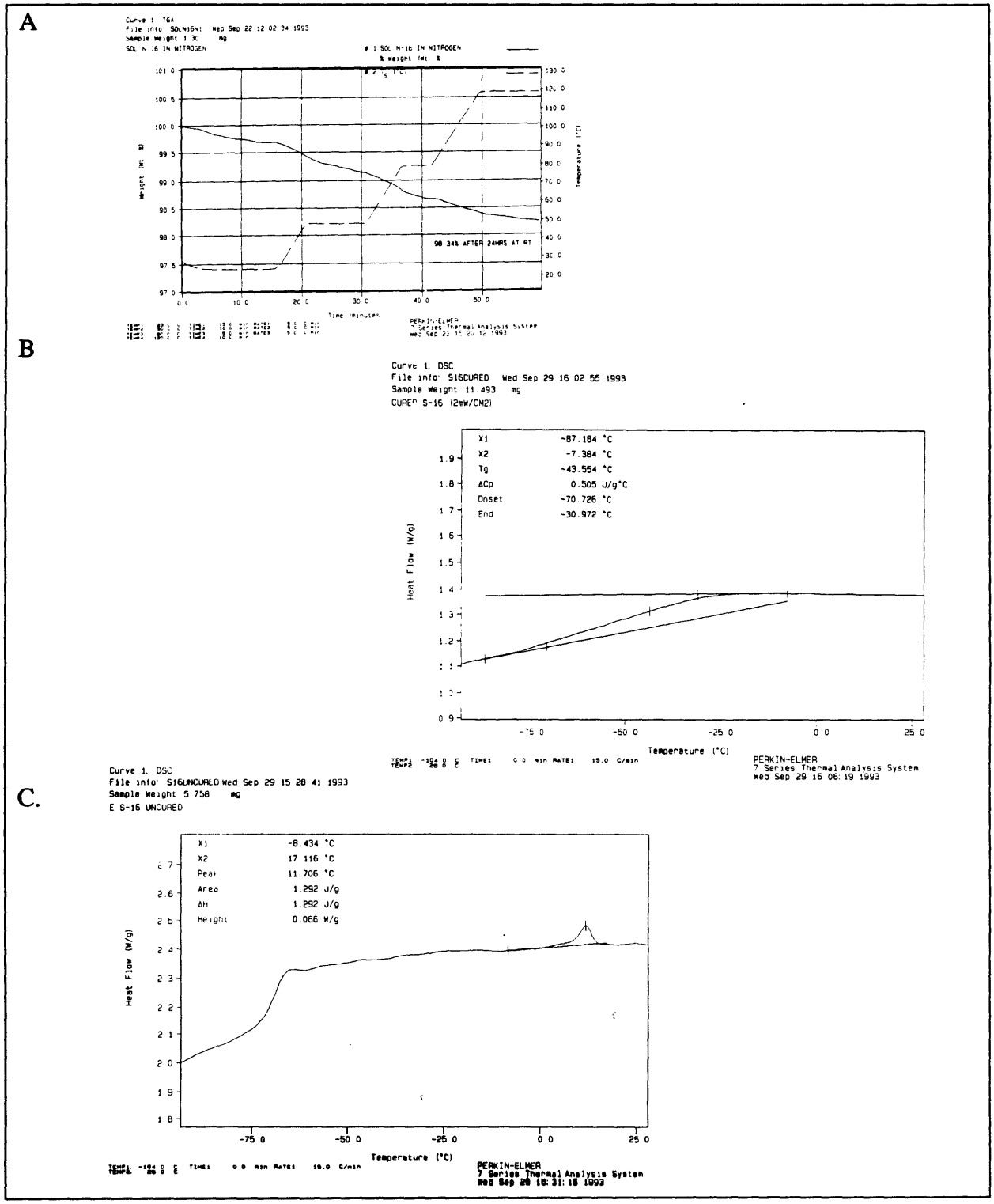

Figure 4-1. Characterization results.[41] **A:** Thermogravimetric analysis. **B and C:** T_g measurement by DSC for fully uncured and fully cured system, respectively.

model predictions to modulus data for the model system. More will be discussed about determining the impurity concentration in Section 4.3.1.

4.1.2 Difunctional Oligomer

Mn of 3500 (+/- 10%) was calculated from high resolution C NMR data by comparing integral values of the poly-ether resonances. A 2.3 wt.%. monofunctional acrylate impurity in the form of 2-hydroxyethylacrylate (2-HEA) was also detected. In using the model to calculate the expected cross-link density and fit predictions to experimental data, the 2-HEA impurity was taken into account as functionally equivalent to the bulk of the monofunctional acrylate.

4.1.3 Monofunctional/Difunctional Solution with Photo-initiator in the Uncured and Cured States

Parameter *af* was calculated for the composition given in **Figure 3-1.** As discussed above, account was taken of both the monoacrylate impurities within the diacrylate, and the estimated concentration of the assumed diacrylate impurity within the monoacrylate. After taking the two impurities as functionaly fully equivalent to the bulk of the monacrylate and diacrylate components, af was determined to be =0.189.

No phase separations were observed for any of the solutions at the polymerization temperature range of interest in this study (>30°C). An interesting finding is represented by the endotherm around 15°C as shown in **Figure 4-1A**. Considering the fact that the particular test sample used was six weeks old at the time of the test, it is possible that the endotherm represents some phase separation even though no cloudiness was observed in that case. Some cloudiness was observed, however, in samples left for a couple of months below room temperature, suggesting that the diacrylate oligomer may have had crystalized out of solution. In any case, the possibility of a phase separation occurring around 15°C should not interfere with polymerizations above room temperatures in which there is no indication of anything but perfect mixing of the two components.

Figure 4-1A shows results obtained from thermogravimetric analysis in which the monomer solution was subjected to a temperature cycle ranging from 0°C and up to 120°C for the last ten minutes of the run. The sample weight loss of <2% during the entire 60 minute cycle and the loss of <0.5% during the 10 minute period at 120°C,

strongly suggest a high resistance to evaporation due to the relatively high molecular weight composition of the components. It should be noted that during a typical thin film photo-polymerization experiment, the monomer solution is exposed to the atmosphere for less than a 15 minute period. Even though the irradiated film is subjected to some convective flow from the steady $N_{2(g)}$ circulation, this additional factor, (which is not present in the thermogravimetric experiment), is not expected to increase total evaporation during photopolymerization to levels above the 2% thermogravimetric finding, even for reaction temperatures around 120°C. A potential concern, however, is that a considerable fraction of the original 0.1% photo-initiator concentration is lost during the overall negligible evaporation. A high enough evaporation rate of the photo-initiator would invalidate the constant R_i assumption. The kinetic data shown in section 4.2 validate the presence of a sufficiently constant R_i throughout the polymerization reaction.

Figures 4-1B and 4-1C give DSC results for measuring T_g of the monomer solution and of a fully cured film, respectively. A few typical trends are readily observed from comparing the plots: As the conversion level increases, T_g shifts to higher temperatures, ΔC_p decreases and the glass transition spreads. Most important is the fact that even the fully cured sample has a low enough T_g (-43.5°C) so that one can be confident that the polymerization takes place well above T_g for the temperatures around room temperature and above. For these temperatures, the relatively low T_g characteristic strengthens our confidence in the assumption of no diffusion controlled kinetics throughout the bulk of the polymerization.

4.2 Kinetics (and Thermodynamics) of the Free Radical PhotoPolymerization

Figure 4-2 shows a logarithmic plot of residual acrylate percent, 100(1-*p*), as a function of irradiation time for a given irradiation intensity (2.5 mW/cm^2) and for different polymerization temperatures. The data were obtained from NIR measurements as discussed earlier. From **Equation 2-3** it can be shown that the shape of the curves in **Figure 4-2** is expected to be linear (first order in acrylate concentration) with an absolute value of the slope equal to $(R_i/2K_t)^{1/2} K_p$ following the assumptions of the steady state free radical photo-polymerization mechanism. Given R_i, which presumably can be determined and controlled independently of the polymerization temperature, the slopes of the curves in **Figure 4-2** can be used to determine the ratio $K_p/K_t^{1/2}$ as a function of polymerization temperature.

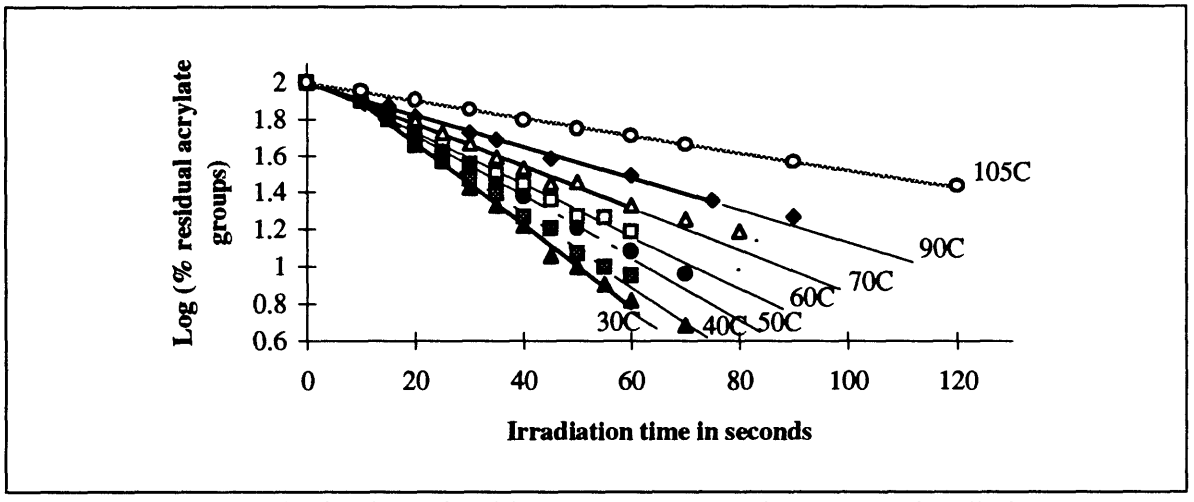

Figure 4-2. Logarithmic plots of residual percentage acrylates versus irradiation exposure time (2.5 mW/cm^2) for different polymerization temperatures. Under the assumptions of the free radical photopolymerization mechanism, the plot should be linear with an absolute value slope equal to $K_p(R_i/2K_t)^{1/2}$.

Measurement of R_i according to the procedure listed in **Appendix A** yielded an estimated value of (5.1 x 10^{-6}) molar/s (+/- a factor of <10).

As shown in **Figure 4-2**, typically, the data deviates from the dominating linear portion of the curve during the very early and very late stages of the polymerization. In these two regions, the rate of polymerization is below the rate indicated by the dominating slope. The initial slow rate, the so called induction period, is most probably attributed to the building up of a steady state radical concentration against the presence of radical scavengers, mostly dissolved oxygen, and inhibitors present in the commercial monomers. The disappearance of this region at the higher polymerization temperatures could be explained by improved oxygen diffusion out of the sample during the period of exposure to N_2(g) flow prior to the irradiation.

The substantial decrease in the reaction rate during the polymerization of the last 10-20% of residual acrylates is most probably attributed to increasing restrictions on the mobility of radicals and acrylates connected to the network as a result of the strongly increasing crosslinking density as the reaction approaches full conversion . One can also notice that as the polymerization temperature increases, the region of decaying polymerization rate starts at relatively lower conversion levels. This finding is inconclusive, especially in light of an unlikely explanation according to which, with the increasing termination rate

constant at higher polymerization temperatures (see following discussion), the termination step is (somehow) less affected by the cross linking density than the propagation step. The possibility that at high polymerization temperatures the slowing of the reaction rate is due to loss of photo-initiator (by consumption and/or evaporation) has been experimentally eliminated.

4.2.1 Polymerization Kinetics as a Function of Temperature

Since the above discussed deviations do not affect significantly the bulk of the polymerized sample, the most obvious and interesting trend from the kinetic view point is the clear decrease in the rate of polymerization (kinetic curves in **Figure 4-2** become more horizontal) with increasing polymerization temperature (above 30°C) for a given initiation rate. **Table 4-1** gives the absolute values of the (least square fitted) slopes ($x10^4$) for each polymerization temperature. For example, the slope (which is proportional to $K_p/K_t^{1/2}$) decreases by a factor of 2.6 as the polymerization temperature increases from 30°C to 90° C. The overall rate of polymerization decreases with temperature since $K_t^{1/2}$ increases faster with temperature than K_p does. **Figure 4-3** (on the next page) is an Arrhenius plot giving the natural logarithm of the absolute value of the slopes ($x\ 10^4$) of the kinetic curves vs. the reciprocal of their respective polymerization temperature (in Kelvin). According to the Arrhenius model represented by **Equation 2-8**, the slope of this presumably linear relationship equals $(1/2E_t-E_p)/R$ (where we assume $A_{td}=A_{tc}$ so that E_t, the general termination activation energy, represents either E_{tc} or E_{td} depending on which is the smaller, or which dominates the termination mechanism). A least square fit to the data between 30°C and 90°C gives $E_p-(1/2)E_t=-14.6$ kJ/mole.

Table 4-1

Absolute value of the (least square fitted) slopes ($x10^4$) of the kinetic curves (see Figure 4-2) for different polymerization temperatures

Polymerization temperature (°C)	$10^4(R_i/2K_t)^{1/2}\ K_p$
20	215
30	223
40	193.1
50	165.7
60	154.8
70	115.3
90	85.9
105	47.8

The data point at 20°C was not included in this analysis due to its proximity to the temperature at which phase seperation was observed, (and consequently the poor fit to the expected first order kinetics in acrylates.) It is conceivable that a maximum rate (which has been observed in other studies) occurs somewhere between 20°C-35°C, however, we shall not be concerned with this finding in this study which focuses on polymerization temperatures above 30°C in order to avoid a more complicated regime of the kinetics and network development. The data point at 105°C was also not included in the least square fit due to the obvious deviation from the linear trend. Again, this deviation demonstrates some of the complexities involved in studying the temperature dependence of bulk polymerization kinetics. A general explanation for this deviation is that it may represent a shift to another kinetic regime in which the activation energy for termination is substantially lower as a result of the overcoming of some energy barrier limiting the termination rate constant at temperatures below 100°C.

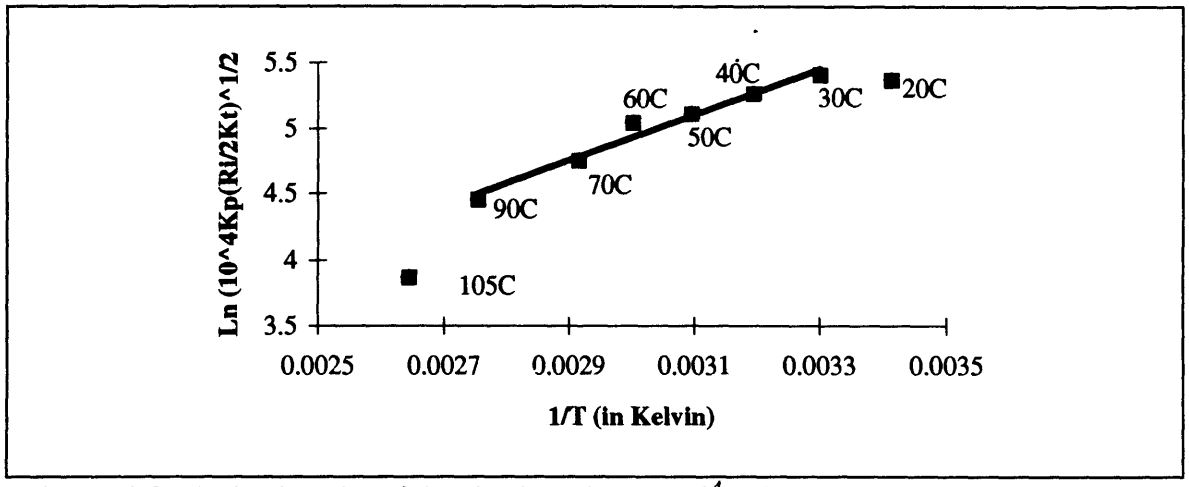

Figure 4-3. Arrhenius plot of the absolute slope (x 10^4) of the rate curves vs. the reciprocal of their respective polymerization temperature (in Kelvin). The slope of the fitted linear curve between 30°C and 90°C is expected to equal $(1/2E_t - E_p)/R$, where E_t is the is the dominating termination activation energy in that temperature regime.

The finding of a significantly negative apparent E_p-1/2E_t value stands out when compared to existing data in the literature where E_p-1/2E_t is a positive quantity (typically on the order of 10-20 kJ/mole) for different monoacrylates and methacrylates polymerized in solution at a polymerization temperature range of 60°-160°C.[32] While there also exists a body of literature concerned with the polymerization temperature effects on the kinetics of crosslinking polymerizations, in these studies, the systems of interest were of relatively high T_g, and were polymerized at temperatures close to or below the T_g and/or other transition temperatures (such as crystalization temperatures) of the monomers and polymer.[5,33,28,34,35] The focus there was on the diffusion controlled regimes of termination (Trommsdorff effect and radical trapping), propagation, and even initiation. Naturally, in these systems, the overall polymerization rate increased with polymerization temperature (up to temperatures in which depolymerization kicked in), and significant deviations from the steady state assumptions were observed.

It is difficult to establish the relevance of data from the above studies to the low T_g crosslinking model system polymerized relatively high above the T_g of the polymer network as in this study. There is no doubt, however, that the deviation from steady state kinetics close to full conversion is attributed to restricted mobility caused by the densely crosslinked network. As the final 10-20% of residual acrylates are polymerized, it is expected that even the propagation step is affected by limited mobility of radicals and

acrylates. The question remains as to what mechanism explains the apparent stronger increase in $K_t^{1/2}$ relative to K_p during the polymerization up to 80-90% conversion with increasing polymerization temperature. The key, is to realize that, E_t, the dominating termination activation energy, seems to be associated with the mobility of the radical, while E_p, the propagation activation energy, is probably dominated by the chemical reaction itself.

One explanation, therefore, is that as we increase the polymerization temperature, we reduce the viscosity (and, increase temperature distance above T_g) of the system, thus increasing the mobility of the radicals and consequently the termination rate constant. This explanation is unlikely, however, since the viscosity increase as a function of conversion, at a given polymerization temperature, is orders of magnitude larger than the viscosity difference as a function of temperature in the range explored, and yet we do not observe autoacceleration (Trommsdorff effect) which is common in bulk polymerizations and often correlated with viscosity. An experimental result confirming the above disqualifying explanation was the photo-polymerization of the low viscosity monoacrylate by itself. It was found that the kinetic behavior with polymerization temperature was essentially identical to that of the monoacrylate/diacrylate system, indicating that the increased mobility of the radicals did not correlate with the viscosity of the system. The same disqualifying explanation is valid with regard to the increase in T_g of the network as a function of conversion. The increase in T_g with conversion can easily exceed the increase in distance from T_g with increasing polymerization temperature and yet again no autoexcelleration is observed in the overall rate of polymerization. Based on this realization, it can be suggested that the relaxation mode of the radical correlating with the bimolecular termination rate involves a shorter time scale than that associated with T_g, or the viscosity for a given conversion level. This suggestion of a short range interaction (probably less than ten carbons) for termination requires further investigation, since existing studies correlate the diffusion controlled termination with distance from T_g, and viscosity, which is doubted to be the case here.

A different mechanism for increasing radical mobility with increasing polymerization temperature is chain transfer by a high mobility transfer agent. Under the assumption that the transfer step is at least as fast as the propagation step, the steady state model predicts that transfer would have no effect on the overall polymerization rate. However, considering that in a bulk crosslinking polymerization, the mobility of the crosslinked (and

even uncrosslinked) polymer radical is substantially lower than that of a small free molecule serving as a transfer agent, increasing the polymerization temperature would increase the apparent mobility of the radical indirectly by increasing transfer.[xvi] As a result, K_t is effectively increased, and the steady state approximation applies up to a critical conversion between 80-90%. This mechanism is supported by data showing a substantial reduction in the kinetic chain length with increasing polymerization temperature, a result which is attributed to transfer (see discussion in Section 4.3.2). It is difficult, however, to reconcile this kinetic mechanism with the finding that as we increase the polymerization temperature, the conversion at which the rate shows a substantial decay (breaking of the rate curve) becomes lower. One would expect the opposite: as propagation at high conversions is hindered by the restricted mobility of the entangled and crosslinked polymer radicals, the increased mobility due to transfer would enhance propagation at high conversions for elevated polymerization temperatures.

A thermodynamic explanation for the decreasing polymerization rate with increasing temperature has been proposed in some studies.[28] According to this explanation, the depolymerization reaction becomes significant at high enough temperatures and conversion levels, resulting in an equilibrium amount of residual acrylates. Quantitatively, for the acrylate systems studied in Ref. 29, this phenomena significantly affects the overall kinetics only at temperatures above 150°C, and at 100°C the equilibrium residual acrylate concentration was less than 1%. Therefore, it is most likely that the extremely slow kinetics at high polymerization temperatures at high conversions as observed here is essentially strictly kinetic and not partly a thermodynamic phenomena.

[xvi] The apparent increase in K_t as a result of transfer can be rationalized in several ways (which are not mutually exclusive). First, the mobilization (or remobilization) of the radical via a transfer agent can be vied as if there is translational motion of the radical super-imposed on its localized and constraint diffusive-type mobility which dominates its termination rate. This translational component can be vied as an added extrinsic mobility increasing K_t. Secondly, by transferring the radical to monomers and/or less constraint polymer segments, the mobility of which is higher, the "averaged K_t" would be expected to increase. This explanation is most intuitive, since increased transfer normally results in shorter, and thus less constrained propagating chains, so that transfer may indirectly correlate with the intrinsic termination-related radical mobility, as well as with extrinsic an added extrinsic component.

4.2.2 Kinetics as a Function of Irradiation Intensity

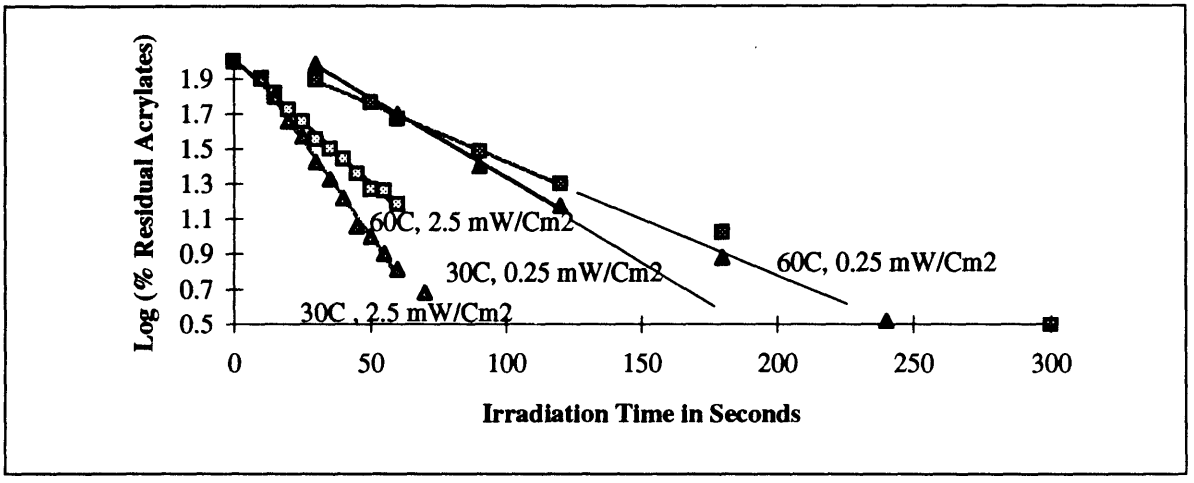

Figure 4-4. Logarithmic plots of residual percentage acrylates versus irradiation exposure time (2.5 mW/cm^2) for two different irradiation intensities at two different polymerization temperatures. Under the assumptions of the free radical photopolymerization mechanism, the plot should be linear with an absolute value slope equal to $K_p (R_i/2K_t)^{1/2}$.

Figure 4-4 shows rate curves for 30°C and 60°C polymerizations, each of which performed at two different irradiation intensities of 2.5 and 0.25 mW/cm^2, respectively.[xvii] Qualitatively, one can observe the increase in the induction period as a result of the decrease in the initiation rate. The change in the absolute value for the slopes as a result of reducing the irradiation intensity, was a reduction by a factor of 2.4 and 2.9 for the 30°C and 60°C polymerizations respectively. By combining **Equations 2-1** and **2-3**, one expects the absolute value of the rate curve slopes to vary in direct proportion to the square root of the irradiation intensity. Thus, since the intensity has been reduced by a factor of 10 in the examples above, one expects the slope to decrease by a factor of 3.3. The deviation of the data from this expectation can be partly explained as a result of the non perfectly uniform reduction in the irradiation intensity at different wavelenghs, given the non uniform photo-initiator absorbance within the irradiation spectrum. The smaller rate reduction with decreasing irradiation intensity for the 30°C polymerization compared with that for the 60°C polymerization is inconclusive, and may be within the experimental error. Additional work needs to be done to get more accurate data of the polymerization kinetics as a function the irradiation intensity. For example, it may be useful to account for the non-uniform reduction in the irradiation spectrum intensity by the (supposedly) neutral density filter. In any case, as will be discussed in Sections 4.3.4 and 4.4 (error

[xvii] A 10% neutral density filter was used to reduce the irradiation intensity by a factor of about 10.

analysis), the qualitative observation of the kinetics as a function of irradiation intensity as discussed here for polymerization temperatures of 30°C and 60°C, is sufficient for purposes of understanding the crosslink density data as a function of irradiation intensity.

4.3 Modulus Results

4.3.1 Modulus as a Function of Conversion

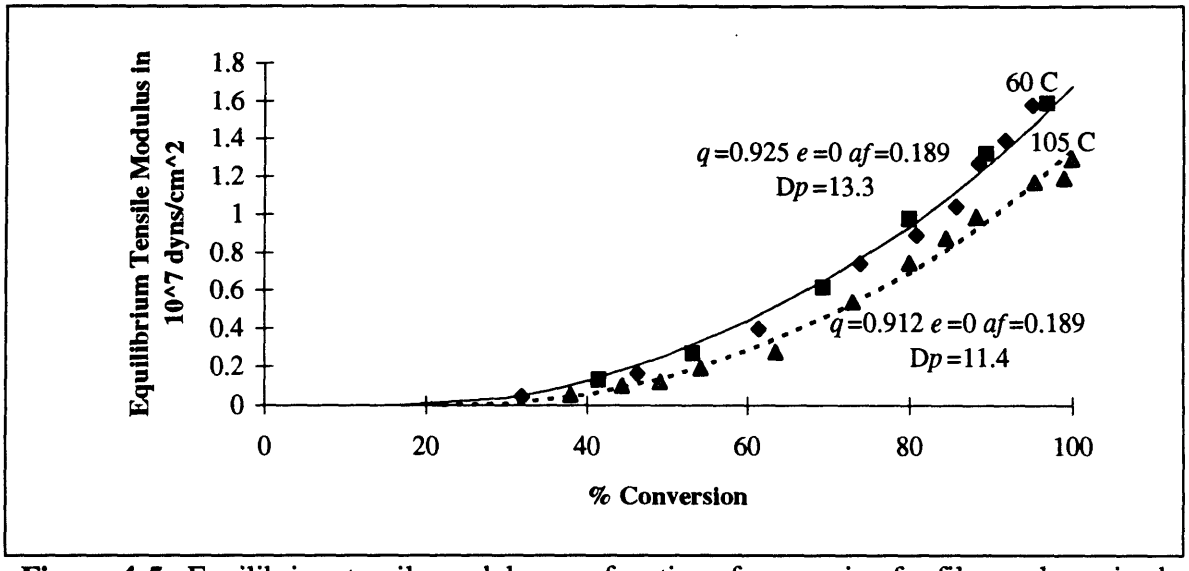

Figure 4-5. Equilibrium tensile modulus as a function of conversion for films polymerized at 60°C and 105°C, respectively. The ▪ and ◆ shapes of data points for the samples polymerized at 60°C represent two different irradiation intensities of 2.5 and 0.25 mW/cm^2, respectively. Films cured at 105°C were irradiated with a 2.5 mW/cm^2 intensity. The continuous curves are the statistical model predictions generated by fitting appropriate q values to the data, while using af=0.189, R_i=5.1 x 10^{-6} molar/s, and assuming e=0.

Figure 4-5 is a plot of the equilibrium tensile modulus as a function of conversion for films polymerized at 60°C and 105°C, respectively. The ▪ and ◆ shapes of data points for the samples polymerized at 60°C represent two different irradiation intensities of 2.5 and 0.25 mW/cm^2, respectively. Films cured at 105°C were irradiated with a 2.5 mW/cm^2 intensity. The continuous curves are the statistical model predictions generated by fitting

appropriate q values to the data, while using $af = 0.189$, $R_i = 5.1 \times 10^{-6}$ molar/s, and assuming $e=0$.[xviii]

Qualitatively, one should notice that the overall shape of the equilibrium tensile modulus (and therefore crosslink density) as a function of conversion has a clear positive curvature to it as predicted by the recursive model for changes in the cross-link density with conversion. Generally, for a given af value, the modulus data show a stronger curvature than that predicted by the model when fitting the appropriate q and e values. A particularly strong deviation occurs at "100%" conversion. It was found that when films are irradiated for extended periods beyond the point of "full conversion" as measured by the NIR method, their modulus jumps to an "above full conversion" level by 5-15%. This jump obviously cannot be predicted by the smooth curve generated by the model. The deviation toward a stronger positive curvature than predicted can have several explanations:

1. If the reactivity of the monoacrylates is higher than that of the diacrylates, more crosslinking reactions will take place during the late stages of the polymerization. This would tend to keep the crosslinking density as a function of conversion below the expected values in the low conversion region while increasing it steeply as the last 30-40% react.

2. It is conceivable that in actuality, af is larger than the value used here to fit appropriate q and e values (or equivalently, D_p). In this case, a larger af value and a smaller q would be required to predict the observed modulus data for a given conversion. As discussed in Section 2.6.1.5, the smaller q, the stronger the positive curvature of the modulus as a function of conversion. The reason for a possibly inaccurate af value resides in estimating the diacrylate impurity concentration within the monoacrylate. In order to use the model to back calculate the diacrylate concentration from the modulus

[xviii] .Attempts to simultaneously fit the independent rate constant activation energies and prefactors based on both kinetic and modulus data as a function of polymerization temperature and given estimated R_i (while assuming 50% termination by combination) under the assumption of no transfer, have failed for reasons explained later on. The assumption of $e=0$, thererfore, reflects the high R_{tr}/R_i ratio so that the crosslink density as a function of conversion, initiation rate, and polymerization temperature is dominated by q, which also dominates D_p, and which does not correlate directly with the observed overall polymerization rate changes with R_i and T. The q/e composition effect on the crosslink density for a given conversion and D_p was briefly explained in Section 2.5. From the explanation it is apparent that in this case of large R_{tr}/R_i, D_p can be accurately directly correlated with the crosslink density under the assumptions of the model, and by plugging $e=0$.

data of the monoacrylate polymerized by itself, q is required (neglecting e), however, q can be calculated by the model only given af. A possible solution would be to try several concentrations of the diacrylate oligomer mixed with the monoacrylate, and by measure the modulus of these formulations polymerized under identical conditions at a given conversion. One could than use that data to fit simultaneously q and af under the assumption that q is sufficiently independent of the formulation.

3. The presence of any impurity serving as an effective crosslinker or more generally any crosslinking reaction which has not been accounted for, would tend to increase the curvature for the same reasons discussed above.

It should be also pointed out that the accuracy level with which the conversion is determined by NIR spectroscopy decreases towards the final percentages of residual acrylates, as signal to noise ratio decreases. Therefore, it is conceivable that the jump in the post "full conversion" modulus is merely an experimental artifact, regardless of the general deviation toward high curvature which could be attributed to any combination of the reasons discussed above. For this reason when fitting q and e to modulus data, a higher weight was attributed to data obtained at conversion levels between 60-90%. At conversions below 50%, even though the conversion level measurement is reliable, equilibrium tensile modulus measurements tend to be less reproducible than at higher conversions. That is why the 60-90% conversion regime is probably the optimum for fitting model predictions with experimental results.

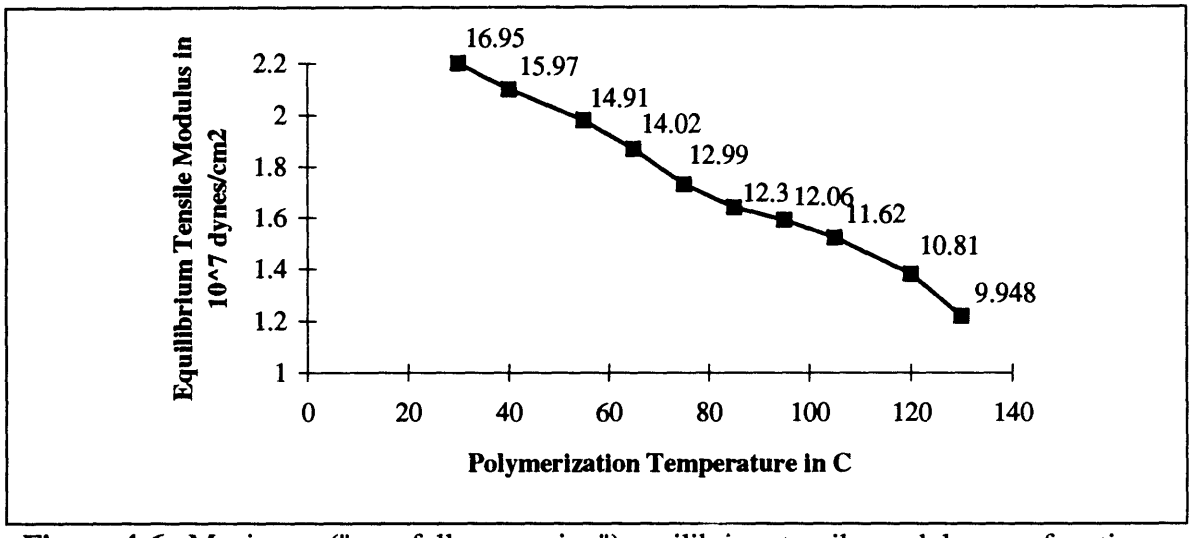

Figure 4-6. Maximum ("post full conversion") equilibrium tensile modulus as a function of the polymerization temperature. Numerical values by the data points represent D_p as calculated from the model predicted q for full conversion, *af*=0.189, and using *e*=0.

4.3.2 Modulus as a Function of the Polymerization Temperature

Figure 4-6 gives the maximum equilibrium tensile m odulus as a function of the polymerization temperature. Here, the maximum modulus is defined as the "post full conversion" modulus which was achieved by irradiating the fully cured films (according to NIR) for an additional 10 minute period at 30°C. The reason for the additional irradiation at 30°C was to guarantee maximum (and thus equal) conversion of all films, especially those cured at temperatures above 100°C which may have some residual equilibrium acrylate concentration. Ideally, one would like to have data showing a continuos series of modulus as a function of conversion curves for all polymerization temperatures similarly to the data shown in **Figure 4-5** for 60°C and 105°C. Unfortunately, the limited sensitivity of the modulus measurement at low conversion makes this unfeasible due to large number of required data points for each, say, 10° interval. Also, as mentioned earlier, the choice of full conversion modulus is advantageous to appreciate the effect of polymerization temperature due to the diverging nature of the modulus as a function of conversion curves.

A potential problem with using the maximum modulus data is that it may include some additional crosslinking which are not accounted for in the model, as mentioned earlier. However, since the assumed additional crosslinking is relatively small (5-15% of the "full

conversion" crosslinking), and since it seems to affect all films about equally regardless of their polymerization temperature, it allows for a valid appreciation of the polymerization temperature effect on the crosslink density for a given conversion level. It also may be the case that, the maximum modulus data is, in fact, the most accurate indication of the true full conversion crosslinking density. In any case, from an application's perspective, the maximum modulus data would usually be a most important material's parameter for the manufacturer, as it embodies an upper limit value for a fully cured system under given processing conditions such as the polymerization temperature discussed here.

Figure 4-6 shows the strong monotonic decrease in the equilibrium tensile modulus with increasing polymerization temperature.[xix] The full conversion modulus or crosslink density is almost halved as the polymerization temperature increases from 30°C to 130°C. A control experiment was set up to check whether the influence of the elevated polymerization temperature was strictly associated with the polymerization kinetics, or could also involve some other irreversible physico-chemical changes which affect the measured modulus in a manner not accounted for in our model (evaporation of photo-initiator is one example). It was found that films subjected to a heating cycle in which they were elevated to temperatures above 100°C for 10 minutes and than cooled down to a lower temperature at which they were fully cured had modulus values corresponding to the polymerization temperature irrespective of their temperature history prior to the irradiation. Thus, the control experiment supported the underlying notion that the polymerization temperature in the range explored affects the crosslink density directly via changes in the free radical kinetics of the system, and so it validates the use of the statistical model as a tool to analyze the relationship between the modulus and the polymerization temperature. The following analysis, will therefore assume that no temperatures effects outside the free radical kinetic mechanism and recursive network model assumptions are responsible for changes in the crosslink density as a function of the polymerization temperature in the range of interest.

As previously discussed, changes in the crosslink density with polymerization temperature can be attributed to a combination of simultaneous changes in the different rate constants

---

[xix] Ref. 2, a rather qualitative study, points out a similar reduction in the modulus with increasing photopolymerization temperature for a low T_g polyurethane, acrylate fiber optic, UV curable system. The authors propose that the reduction in the crosslink density was due to an increase in the termination rate relative to propagation, and an increase in the degree of termination by disproportionation. In this more quantitative study, it is shown that neither of these explanations holds valid for the system investigated here.

that control the overall kinetics and therefore the network structure. Ideally, one would need to measure each of these individual rate constants as a function of temperature in order to have a complete picture of the overall changing kinetics and the determination of network structure with temperature based on the set of model assumptions. This kind of approach is often not feasible, and generally is unnecessary for purposes of gaining an understanding of the dominating effects on cross-link density or D_p with polymerization temperature.

Using the model to illustrate the relationship between the crosslink density and the measured equilibrium tensile modulus, the predicted D_p values were back calculated (by finding q for full conversion, e=0, and af=0.189) and are presented in **Figure 4-6** next to the corresponding modulus data points. According to the model, D_p is shortened from about 17 at 30°C to about 10 at 130°C. This decrease in D_p can be explained by the model as the result of a decrease in q, e, or in both.

As discussed in Section 2.6.1.1, the conditions under which a switch from termination by combination to termination by disproportionation would explain the observed reduction in D_p with polymerization temperature are the presence of a combination of sufficiently small R_{tr}/R_i and q values. For D_p values between 10 and 17, q would be between 0.942 and 0.899 for e=0 (no combination), and af=0.189. Looking at **Table 2-1**, a $R_{tr}/R_i > 10$ would restrict the influence of parameter e in determining the crosslink density to <7%, and a $R_i/R_{tr}>100$ would restrict its influence to within <1%. Having already calculated R_i independently to within an accuracy of a factor of 10 (or less), and using the values for $K_p/(2kt)^{1/2}$ as obtained from the kinetic study, one has to conclude (based on **Equation 2-6**) that $R_{tr}/R_i > 10$ for polymerization temperatures as high as 130°C and that $R_{tr}/R_i>100$ for polymerization temperatures around 30°C. If we were to assume, for example, that no transfer is present, based on the kinetic data, we would obtain an average D_p value on the order of 10^3-10^4 (depending on the polymerization temperature), which is obviously not the case. Also, based on **Equation 2-6** , for sufficiently low R_{tr}/R_i ratios, one would expect to observe the effect of the initiation rate on D_p and thus on the modulus, especially for the elevated polymerization temperatures where D_p is lower to begin with. As will be shown later, this is not the case. Thus, we can eliminate the possibility that changes in parameter e, or that a shift from termination by combination to termination by disproportionation is the cause of the decrease in crosslinking density with increasing polymerization temperature.

Having eliminated *e* as an option by realizing its restriction to values close to 0 in the polymerization temperature range explored, one needs to focus on a decrease in *q* as the dominating cause of the decreasing crosslink density with polymerization temperature. Ideally, for the case of negligible transfer, one would use the kinetic information showing the decrease in overall polymerization rate with temperature to independently obtain *q* as a function of temperature for given *e*, *af*, and R_i values. In this case, however, we have already shown above that transfer plays a dominant role in determining D_p, since, when assuming negligible transfer, the overall kinetics predict D_p values which are 3-4 orders of magnitude greater than the experimental data. Yet, the kinetics also clearly indicate a substantial decrease in the overall polymerization rate with increasing polymerization temperature. The issue, therefore, is weather or not it is possible to establish a direct relationship between *q* (and thus the crosslinking density) with temperature and the overall kinetics with temperature. Qualitatively, under the assumption of constant initiation rate as a function of temperature, the dominating increase in the termination rate constant over that of the propagation constant with temperature as earlier discussed would tend to reduce *q*. Quantitatively, however, the presence of significant transfer dampens this effect as can be seen from **Equation 2-6**. Thus, the fact that transfer affects the overall polymerization rate indirectly makes it is impossible to establish a direct connection between the kinetic data form **Figure 4-2** and the full conversion equilibrium tensile modulus data from **Figure 4-6**.

For demonstration, lets consider the reduction in $K_p/K_t^{1/2}$ by a factor of about 2 as a result of increasing the polymerization temperature from 60°C to 90°C (see **Table 4-1**). If transfer could be ignored, one would expect a reduction by a factor of almost 2 in D_p, assuming no change in the dominating termination mode (represented by *e*, or ω in **Equation 2-6**.) **Figure 4-6**, shows that the reduction in D_p is by less than 20%. Naturally, one has to realize that a less than 20% reduction in D_p under conditions of dominating transfer (as in this case) affects the modulus much more dramatically than reduction by a factor of 2 would under the assumption of no transfer. In the latter case, using the kinetic data alone, D_p would be so large (10^3-10^4) that a factor of 2 reduction in its value would hardly be noticed in the measured modulus. A look at **Equation 2-9** also shows that assuming chain transfer to account for the overall low D_p, while equating E_{tr} and E_p, so that the reduction in D_p with polymerization temprerature is explained by the dominating increase in the termination rate constant (due to the negative $(1/2E_t-E_p)$)

cannot quantitiatively explain the D_p reduction as a function of polymerzation temperature This realization was further supported experimentally by the absence of a notable irradiation intensity effect (see next section) on D_p. One has to conclude not only the presence of dominating transfer in the system, but also that the increase in the transfer rate constant with temperature is the dominating cause of the observed reduction in the crosslink density with increasing polymerization temperature.

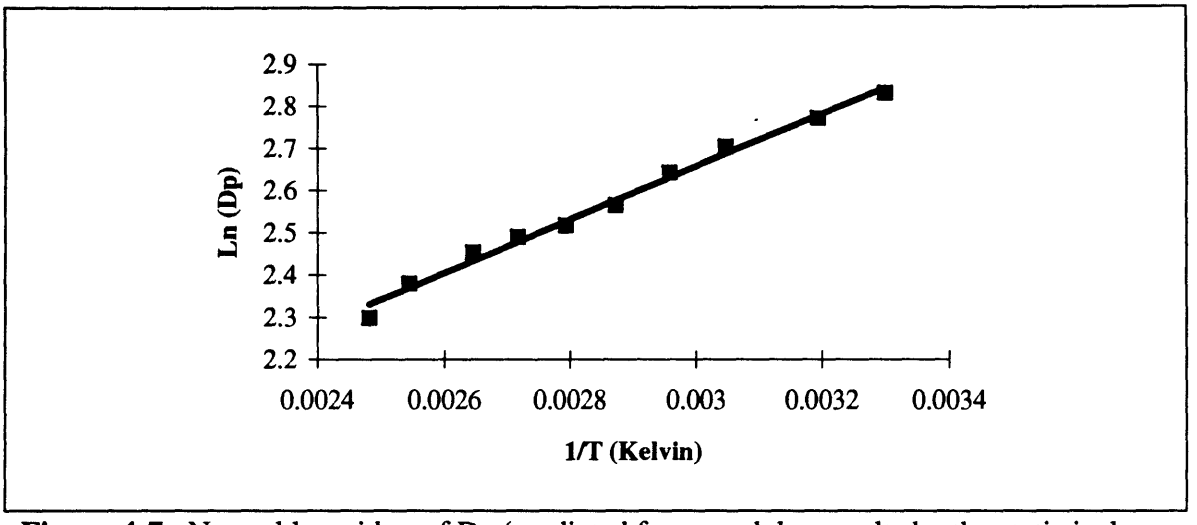

Figure 4-7. Natural logarithm of D_p (predicted from modulus results by the statistical model for full conversion, *af*=0.189, and e=0) vs. the inverse of the polymerization temperature in Kelvin.

Figure 4-7 plots the natural logarithm of D_p vs. the inverse of the polymerization temperature in Kelvin. Given that $R_{tr}/R_i>100$, and assuming a single dominant transfer reaction, the slope of this presumed linear relationship is expected to equal $E_{tr}-E_p$ which in this case gives 5.2 kJ/mole.[xx] This Arrhenius relationship follows **Equation 2-9** for the case in which R_i can be neglected so that the numerator is essentially equal to independent of T (ω=1), and the denominator consists of only a single R_{trx}/R_p term. The positive value of $E_{tr}-E_p$ simply means that the rate of transfer increases faster than the rate of propagation with temperature, which is a necessary condition in order for transfer shorten D_p with increasing polymerization temperature. More experimental evidence of the dominating transfer reaction will be provided in the next section showing the influence of initiation rate on crosslink density as at different polymerization temperatures.

[xx] Future work may quantitatively compare this value to literature data while accounting for the potential transfer agents, their concentration, etc.

Even though the increasing transfer rate with temperature can be well correlated with the decrease in the crosslink density with increasing polymerization temperature, it is not clearly established weather transfer is responsible for the increased mobility of the radicals which is correlated with a decrease in the overall polymerization rate with temperature due to a dominating increase in the termination rate constant. However, the clear evidence of transfer increasing with temperature, may give support to a mechanism earlier mentioned by which the activation of transfer increases the apparent K_t via the mobilization of the radicals. It should also be mentioned that the presence of relatively low D_p radicals (with potentially higher mobility) as a result of the extensive transfer may be another indirect way by which transfer facilitates termination with increasing polymerization temperature.

Since no transfer agent was added as part of the formulation used here, the question to be asked is what component or impurity of the system served as an effective transfer reagent. Since it is expected that transfer to the monomer or polymer would have no significant impact on the crosslink density, especially at full conversion, it is most probably the case that an impurity serves as the transfer agent. This realization is further supported by published data giving negligible transfer coefficients to the monomer and polymer in various acrylate systems. Given that the polymerized monoacrylate by itself shows a similar polymerization temperature dependence of the kinetics and D_p to that of the mono/diacrylate system, it is most probable that the transfer agent served an impurity in the commercially monoacrylate product. This conclusion is supported by the NMR spectrum of the diacrylate oligomer which showed no indication of an impurity which would serve as an effective transfer reagent. Preliminary analysis of the monoacrylate product indicated the presence of a large number of impurities, though it is yet to be determined which may act as the effective transfer agents. The possibilities that the photo-initiator itself and/or inhibitors present in the commercial products may act as transfer agents are less likely to be the case, but not ruled out.

4.3.3 Modulus as a function of irradiation intensity

Figure 4-2 gives the equilibrium tensile modulus as a function of conversion for a 60°C photo-polymerization performed at irradiation intensities of 2.5 and 0.25 mW/cm^2, respectively. As one can see, the two sets of data points are statistically indistinguishable. This result is expected in light of the overwhelming transfer rate which causes $R_{tr}/R_i>100$ at 30°C for a 2.5 mW/cm^2. As the polymerization temperature increases, so does the rate of transfer while the initiation rate is assumed unchanged. Thus, increasing the

polymerization temperature increases the R_{tr}/R_i ratio which in turn further eliminates the effect the irradiation intensity effect on D_p, and therefore, on the crosslink density and the measured modulus.

In order to observe significant changes in the crosslink density with irradiation intensity, one needs to operate in a regime where R_{tr}/R_i is small enough while accounting for the R_p/R_{tr} ratio (or R_p/R_i in the case of $R_i>R_{tr}$). In this case, given $R_{tr}>R_i$, R_p/R_{tr} is between 10-20, and assuming disproportionation as the dominating termination mechanism, a ratio of $R_{tr}/R_i<20$ would be required to observe changes in the modulus with irradiation intensity. If combination serves as the dominating termination mechanism, a ratio of $R_{tr}/R_i<5$ would be required. Taking the transfer rate as fixed for a given polymerization temperature for the system used here, one needs to increase the irradiation intensity by a factor of 100-1000 (depending on the polymerization temperature and the dominating termination mechanism) in order to observe the initiation rate effect on the measured modulus. Alternatively, one could increase the photo-initiator concentration, or choose a combination of both methods to sufficiently increase R_i.

4.4 Error Propagation Analysis

In order to fully account for accumulated errors propagating throughout the gathering of data and up to the analysis of results in this study, we need to consider errors resulting directly from experimental measurement accuracy-limitations, as well as errors resulting from assumptions, simplifications, and approximations made in the theoretical framework, including the statistical model and its calculation. However, in light of the semi-quantitative nature of the results and conclusions obtained, and in light of the emphasis in this study on the kinetics and the kinetic model analysis as a useful tool rather than on the pure quantitative aspects, in this section, the error analysis will also take the form of a semi-quantitative treatment.

The reproducibility of modulus measurements to within less than 3%, essentially eliminates the need to consider implications of this error on the observed dramatic decrease in modulus with increasing polymerization temperature. The assumption of constant average polymerization temperature despite the ≈5°C temperature increase during the polymerization reaction (as a result of the exothermic heat release,) results in negligible error for purposes of establishing a clear trend both in the full conversion modulus and

reaction kinetics as a function of temperature. For both these measurements, the experimental sensitivity easily enabled to resolve statistically significant differences for 10°C intervals in the polymerization temperature.

The combination of errors involving conversion and modulus measurements at relatively low conversions, and the diverging nature of modulus curves with conversion, required an unfeasible number of data points to clearly resolve modulus as a function of conversion curves for polymerization temperatures within 30°C. Nevertheless, for a given polymerization temperature, the shape of modulus as a function of conversion curves was clearly established, and differences in modulus for 5-10% increase in the conversion level were easily resolved, as was the difference between a 30°C and a 105°C modulus as a function of conversion curves.

As can be expected, the least reproducible kinetic results occur at the beginning and end of the polymerization reaction. Fortunately, errors which may lead to inconclusive explanations about the nature of the reaction in those regions do not affect significantly the analysis regarding the kinetic behavior of the bulk 80% of acrylates, and the crosslink density as calculated by use of the model for given conversion and modulus data.

The uncertainty to within an order of magnitude involved in estimating the initiation rate had no effect on model predictions and modulus interpretation due to the overwhelming dominance of the transfer rate. The dominating transfer at all polymerization temperatures was also advantageous in the sense that it relaxed the importance of the temperature and conversion independence of initiation rate assumption as far as the crosslink density as a function of temperature was concerned. As for the temperature dependence of the kinetic data, since the most probable direction in which the polymerization temperature may change the initiation rate is to increase it, the uncertainty in the temperature independent initiation rate assumption, is if anything, is more likely bound to underestimate the extent to which the termination rate constant increases with temperature, rather than overestimate it. Therefore, at least qualitatively, one should be quite confident in the finding that $K_p/K_t^{1/2}$ decreases with increasing polymerization temperature. The rate of polymerization results and UV analysis of residual initiator strongly supported the assumption of constant initiation rate with conversion, at least up to the final 10-20% of unreacted acrylates.

The use of the dominating slope portion of the kinetic curves as a function of temperature to interpret the modulus as a function of temperature data using the statistical model, incurred no error despite the uncertainties discussed above. Again, this is simply because of the dominating transfer which strongly affected the crosslink density directly with temperature, but presumably had a much weaker and indirect affect on the overall polymerization rate as a function of temperature.

Finally, in the statistical model used here, it was implicitly assumed that D_p (or q for that matter) is a constant independent of conversion. In other words, there was no account of the conversion dependent kinetics in the sense that D_p is directly proportional to the unreacted acrylate concentration (**see Equation 2-6**). Under the assumptions of no cyclization and equal and independent reactivity of all acrylates, the distribution of D_p around its average value (at 50% of the conversion level) has an effect on the crosslink density prediction at any conversion. Qualitatively, it is expected that a wider distribution resulting from accounting for depletion dependent kinetics, would increase the crosslink density at any given conversion for a fixed D_p (averaged over the conversion). Therefore, in using the model to predict D_p based on the modulus at a given conversion level, one tends to over estimate D_p. Naturally, the constant D_p approximation also affects the crosslink density as a function of conversion curves, especially during the early stages of gelation in which D_p is close to twice the average value. By use of a conversion-dependent statistical model for the same full conversion crosslink density, the gelation point occurs at an earlier conversion, and the shape of the crosslink density as a function of conversion curve is expected to have a lower curvature relative to the constant average D_p approximation.

The precise quantitative implications of the two errors discussed above, namely the overestimate of D_p (or more directly q while assuming e=0) and the overestimate of the crosslink density curvature with conversion, are rather meaningless when considering the underlying model assumptions of no cyclization, and equal and independent reactivity, in addition to the perfect elastomer behavior assumption. In fact, it was found that when relaxing some of the model assumptions made here, one predicts much stronger effects controlling D_p distribution (in length as well as monomer composition), and thus the crosslink density development than when merely accounting for monomer depletion as a function of conversion. In fact, it is perceivable that the higher than predicted curvature in

the modulus as a function of conversion as found in this study, actually underestimates an even stronger curvature deviation (due to unequal acrylate reactivity, etc.) which is partlycompensated for by the constant average D_p assumption as a function of conversion built into the statistical model predictions used in fitting the data.

Section 5: Conclusion and Recommendations for Future Work

5.1 Conclusions

By employing a simple statistical network model in conjunction with a simple and low cost experimental procedure, we have gained a basic understanding of crosslinking development during a free radical bulk photo-polymerization of a monoacrylate/diacrylate system copolymerized above T_g of the fully cured network. In particular, the effects on the crosslink density of three important processing controlled parameters, namely, the polymerization temperature, the irradiation intensity, and the conversion level, have been investigated both theoretically and experimentally. The effects of a fourth parameter, formulation, as defined here by the monoacrylate/diacrylate concentration ratio was discussed from a theoretical perspective. Some important implications for industrial and commercial applications can be deduced from results obtained in this study:

- The crosslink density, and therefore the modulus, is highly sensitive to conversion, especially during the polymerization of the final 20-30% of residual acrylates. It is therefore pertinent that for applications in which the modulus needs for example to be strictly controlled to within 10% or less, the conversion level is reliably monitored and controlled to within <3-5%, especially for low D_p systems and/or applications in which full conversion is desirable.

- The effect of polymerization temperature on the network crosslink density at a given conversion can be quite dramatic. For polymerization temperatures above T_g of the fully cured network as studied here, it was found that the activation of increased transfer due to an impurity in the commercial monomer product can reduce the full cure modulus by 50% for a 100°C increase. Naturally, a system with a higher concentration of effective chain transfer agents, may exhibit an even more dramatic decrease in the modulus with increasing polymerization temperature. A probable (though inconclusive) side effect of the increased rate of transfer with polymerization temperature was a substantial decrease in the overall polymerization rate, especially during the final stages of the reaction. The reduced polymerization rate may cause

incomplete cure at elevated polymerization temperatures, which in turn would tend to further reduce the modulus. In the general case, changes in polymerization temperature in the regime above T_g of the fully cured network, should be carefully evaluated for their direct effects on the kinetics of the different free radical polymerization reactions, and consequently their effects on the crosslink density and overall polymerization rate. Polymerization temperature effects may be particularly dominating in high cure speed applications in which the combined high rate of exothermic heat generation and direct UV irradiation heating (for photopolymerization) may elevate the polymerization temperature by as much as 100°C during the course of polymerization. High curing speeds in free radical network forming polymerizations characteristically involve high initiation rates which in combination with substantial temperature activated transfer, and incomplete cure (often due to insufficient removal of oxygen from the surrounding atmosphere, for example), may reduce the effective crosslink density by several factors. Sufficient heat transport to control the polymerization temperature of the polymerizing system may, therefore, be an important consideration in the design of a high cure rate system, particularly if full cure is desired at which the modulus should be restricted close to the specified application value.

- Even though the effect of irradiation intensity on the crosslink density has not been directly observed in this study as predicted due to the dominating transfer reaction, under conditions of sufficiently small R_{tr}/R_i and D_p values, increasing the irradiation intensity would reduce the crosslink density dramatically. This reduction in modulus with increasing irradiation intensity should be kept in mind when considering the design of high cure speed applications. Equivalently, increasing the initiator concentration (or photo-initiator concentration as in this case) would also increase the initiation rate which in turn reduces the cross-link density for a given conversion level under the same conditions mentioned for the irradiation intensity effect. One should also keep in mind that increasing the photo-initiator concentration, increases the absorbance which may reduce the network structure uniformity across the sample's thickness. Thus in general, for photopolymerizations, it may be preferable to increase the initiation rate by increasing the irradiation intensity (while controlling the irradiation heating effects) rather than by increasing the photo-initiator concentration.

- Though changing the formulation and composition of the polymer network building blocks, is generally an easy and powerful way to alter the network structure related properties, there are advantages associated with controlling the network structure via direct manipulation of the free radical kinetics. Based on the statistical model, it was shown that for any fixed crosslink density at a fixed conversion, the crosslink density is less sensitive to conversion in a system of high D_p and low crosslinkers concentration compared with a system of low D_p and a high crosslinkers concentration. The reduced sensitivity to conversion close to the full conversion level is important when considering the high probability of incomplete cure occurring as a result of common fluctuations in a variety of processing parameters. It was also shown that a high D_p

low crosslinkers concentration system is expected to be more robust to fluctuations in the free radical kinetics (due to temperature changes for example) affecting D_p, and therefore the crosslink density, compared with a low-D_p-high crosslinker concentration system giving the same crosslink density for the same conversion.

- Overall, on a more general level, the simple experimental and theoretical framework employed in this study, though highly idealized, proved to be useful and implementable for gaining a better understanding of network structure formation and potential ways in which to control the desired structure related properties. It is believed that implementation of similar semi-quantitative (and obviously more quantitative) analytical methods as used here, can have promising contributions to the industrial optimization process of even more complicated network-forming polymerization systems.

In addition to specific findings applicable to processing related control of crosslink density in photopolymerized network forming free radical systems, several findings from this study are worth mentioning as being somewhat more related to fundamental phenomenological aspects. As is often the case, in a study of this nature these curiosities tend to raise more questions than provide clear explanations to some of the observations made:

- The clear first order kinetics, at least during the first 80% of the polymerization, was unexpected in light of the frequently discussed Trommsdorff effect with direct relation to bulk polymerizations as a whole. This finding raises the questions: What is the nature of the rate limiting mobility or relaxation mode required for the bimolecular termination reaction? and How is that mobility affected by conversion and polymerization temperature in the temperature regime above T_g of the fully cured network?

- The mechanism responsible for reducing the overall polymerization rate with increasing polymerization temperature in the regime above T_g of the fully cured network is not clearly understood. Even though it is most probably the direct result of a substantial increase in the termination constant relative to the propagation rate constant, it is only speculated that the increased transfer rate with temperature is indeed responsible for the apparent increase in K_t. Even if it is the case, the mechanism by which transfer increases K_t is also merely a speculation lacking direct experimental evidence.

- Though the substantial decrease in the polymerization rate during the polymerization of the final 10-20% of residual acrylates is not surprising considering the presence of a densely crossed network, there seems to be a correlation between the point at which the rate curve breaks and the polymerization temperature. This correlation (thought inconclusive) raises the question as to what mechanism controls the retardation in the

polymerization rate. In this paper we have made a general speculation that somehow as the polymerization temperature increases the termination process becomes less sensitive to the high conversion relative to propagation. Understanding the direct causes of the slow kinetics toward full conversion may have important consequences for industrial and commercial applications in which high cure speeds and full conversion are often desirable.

- The apparent post "full-conversion" increase in modulus is not clearly understood. Though this observation could be explained as merely an experimental artifact, it may be real. In that case, the questions to asked are: Is the increase in modulus strictly attributed to an increase in the crosslink density? If it is (as is assumed for this system), what is the source for the additional crosslinks (crosslinking impurities or some other effective crosslinking reaction which was not accounted fore)?

- Though, in this study we have been able to use the model as a qualitative and often quantitative tool to explain and predict experimental data, the extent to which the basic assumptions of the model were valid was not clearly established. It would be both interesting and useful to investigate the validity of the equal and independent reactivity assumption as well as assumption of no (or at least negligible) intermolecular polymerization reactions within finite species.

5.2 Recommendations for Future Work

In light of unresolved issues and questions, some of which raised above, this study may serve as a useful starting point for future research work which is expected to build upon the theoretical and experimental strengths of this study while answering questions left open as a result of the existing limitations:

- In order to improve our understanding of the system's free radical kinetics and structural development, it is suggested that individual rate parameters be directly measured as a function of the polymerization temperature. Ref. 24, for example, lists some of the available methods and techniques for independently measuring these quantities using a linear system. Though generally these techniques can be modified for studying non-linear systems while relying on the model, it is suggested that, unlike the commercial monofunctional monomer used here, in future studies, the monofunctional monomer would not crosslink when polymerized "by itself" so that a better evaluation of the crosslinking effect on the kinetics is achieved, and independent data to evaluate the goodness of some of the statistical model and the ideal entropy elastomer assumptions is available.

- Rheological studies and particularly relaxation measurements such as dielectric or DMA are recommended for gaining a better understanding of the mobility rate-limiting mechanisms affecting the kinetics and subsequently the resulting network structure. Specifically the relaxation modes controlling termination as a function of

polymerization temperature should be investigated, and radical mobility possibly correlated with the increase in transfer with temperature.

- In order to gain a better understanding of deviations from model predictions, it is suggested that the goodness of the basic assumptions be directly measured. For example, extraction experiments combined with NMR spectroscopy can be used to monitor the relative consumption of monofunctional and difunctional acrylates as a function of overall conversion. The extent of intramolecular cyclization can be estimated by combining modulus measurements with information about the individual consumption of acrylates diacrylates. Also, combined information about the relative composition of acrylates and diacrylates in the network can be combined with NIR spectroscopy to estimate the independence of reactivity assumption.

- It is recommended that in future studies of network structure formation by free radical polymerizations, a wider temperature, composition, and irradiation intensity range be investigated to study kinetic and other effects at different regimes, such as close to T_g of the fully cured network. It would also be instructive to operate in an irradiation intensity-dependent regime enabling the experimental observation of the initiation rate effect on network structure formation.

- While there is appreciable room for improving and developing additional theoretical predictions and experimental procedures using the simple statistical model of this study, it is also recommended that future studies incorporate newer models which relax some of the basic assumptions made here, and allow for the analysis of more complicated systems. The use of more sophisticated models would naturally require more intensive use of computer software for calculations and simulations. The use of such models may often require kinetic and other parameters in addition to those used here, and concomitantly the quantitative analysis of results would most probably necessitate experimental sensitivity above that achieved here. Recommendations for eliminating some of the errors in this experiment include, improving removal of inhibitors (especially dissolved oxygen at the lower polymerization temperatures), using high purity fully characterized components rather than commercial products of low purity, increasing the initiator concentration while irradiating in a lower absorbance regime, etc.

- Future studies should experimentally investigate model predictions, some of which mentioned in this study, in addition to those tested here. For example, it would be interesting to observe the predicted effect of simultaneously changing q and af on the curvature of the crosslink density as a function of conversion curve. One way of changing q would be to add a controlled amount of chain transfer agents while polymerizing at a fixed temperate and irradiation intensity.

- In this study of network structure development, the main focus was on monitoring crosslink density as measured macroscopically by the equilibrium tensile modulus. It is suggested that future studies employ alternative techniques such as swelling to

independently measure the crosslink density and compare results, at least on a relative scale with equilibrium tensile modulus measurements.Future studies should also include measurement of other model predicted average structural parameters such as the sol/gel fraction, molecular weights of the sol etc.

- Finally, on a most general level, it is suggested that in the future, similar studies be extend to investigate more complex compositions and explore, both theoretically and experimentally, the controll of polymer network structure formation by polymerization mechnisms other than the free radical.

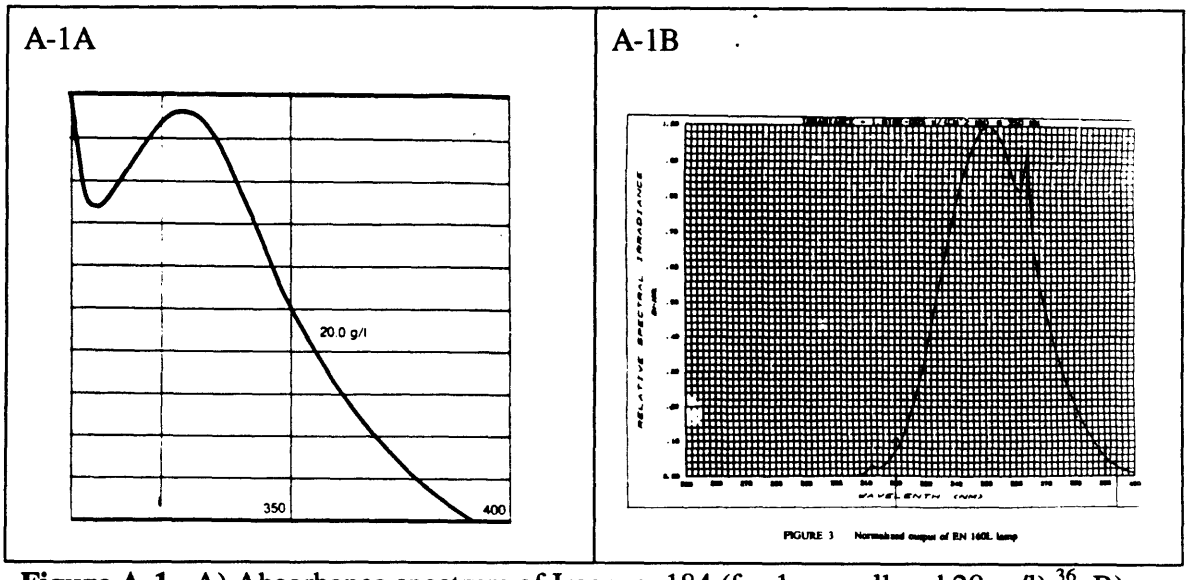

Figure A-1. A) Absorbance spectrum of Irgacure 184 (for 1 cm cell and 20 gr/l).[36] B) Normalized output of EN-160L lamp.[37]

Appendix A: Calculating the Initiation Rate, R_i

K gives the integral sum of the initiator's spectral photonic absorption in moles/(cm Joule). This quantity is directly proportional to the initiation rate as shown in **Equation 2-1**.

$$K = \frac{1000}{A_v hct} \int [\lambda r_{(\lambda)} (1 - 10^{-Abs})] \, d\lambda \qquad \text{(A-1)}$$

where:

$r \equiv$ relative intensity factor

$c \equiv$ speed of light

$h \equiv$ Planck's constant

$t \equiv$ film thickness

The integral in **Equation A-1** was calculated numerically with 2 nm intervals using the values for the photoinitiator absorption (above 320 nm as provided by the manufacturer) and the EN-160L lamp normalized output. In calculating the rate of initiation, the sensitivity of the radiometer as a function of the wave length[1] was also taken into account when determining the irradiation intensity, I_0, at each wave length interval. **Figures A-1A and A-1B** give the absorbance characteristics of the photoinitiator and the relative spectral irradiance of the UV lamp, respectively.

To calculate R_i, one needs the efficiency of chain initiation factor (parameter F in **Equation 2-1**). In this study no direct information about F was available and so F was assumed equal to 0.3. Taking into account the error involved in guessing F, assuming equal reactivity of the two radicals generated by initiation, and other errors in measurements, R_i of (5.1×10^{-6}) was calculated to within a factor of 10. In light of the overwhelming transfer which dominated D_p in our study, the relatively low accuracy with which R_i was estimated did not interfere significantly with the interpretation of modulus and kinetic results in this study. The increase in transfer with temperature also assisted in reducing the importance of the error involved in assuming the polymerization temperature independence of the initiation rate.

Appendix B

A typical NIR difference spectra output (in two different regions) as generated by use of a computer program written by Alex Harris. The cured spectra in the respective regions is used for normalizing thickness variations. At the bottom of **Figure B-1** is the calculated residual acrylate percentage, which in this particular case is 23.2%.

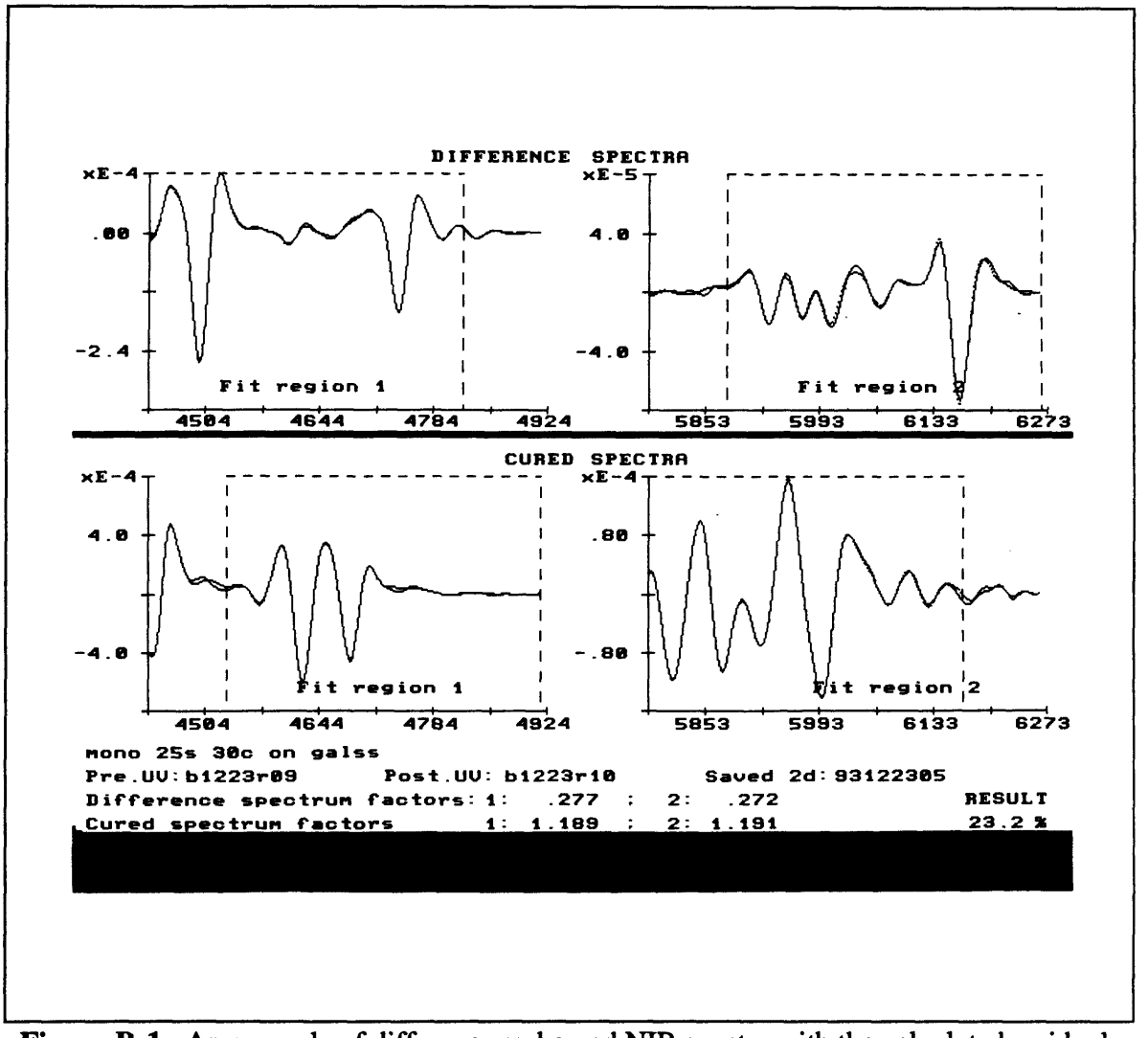

Figure B-1. An example of difference and cured NIR spectra with the calculated residual acrylate percentage by use of a computer program written by Alex Harris.

Appendix C: Model Calculation of Crosslink Density

A brief and simplified summary of the derivation scheme for calculating the network's crosslink density, the average structural parameter of interest in this study, is provided below.

P_{out}, the probability that a crosslinker (a diacrylate in our case) chosen at random from the gel section will have any one of its arms be finite (not extend to infinity) is calculated as a function of q, e, af in a recursive manor, which will not be discussed here. Given P_{out}, the crosslink density is calculated from the probabilities that a randomly chosen diacrylate will have four arms extending to infinity (PX4/4) and the probability that a crosslinker will have only three arms extending to infinity (PX3/4). These two probabilities, which are rather intuitive, are given by **Equation C-1** and **C-2** respectively:

$$PX4/4 = (1- P_{out})^4 \qquad \textbf{(C-1)}$$

$$PX3/4 = 4Pout(1- P_{out})^3 \qquad \textbf{(C-2)}$$

Once PX4/4 and PX3/4 are known, we need to multiply these probabilities by the diacrylate concentration to get the respective crosslink densities, which are then converted in our case to the effective 3-point-crosslink density by use of **Equation 3-2**.

References

[1] Blyler, L.L. Jr., DiMarcello, F.V., Hart, A.C., Huff, R.G. *ACS Symposium Series of the American Chemical Society, Anaheim, CA* **1986**, p. 410-415.
[2] Overton, BJ., Taylor, C.R., and Muller, A.J. *Polymer Engineering and Science* **1989**, 29(17), 1165-1168.
[3] Tobita, H. *Macromolecules* **1992**, 25(10), 2671-2678.
[4] Tobita, H. and Hamielec, A.E. *Polymer* **1992**, 33(17), 3646-3657.
[5] Wight, F.R. *J. Radiation Curing* **1981**, 24.
[6] Nielsen, E.L. *J Macromol. Sci.* **1969**, C3(1), 69-103.
[7] Flory, P.J. *J. Am. Chem. Soc.* **1941**, 63, 3083, 3091, 3096.
[8] Stockmayer, W.H. *J. Chem. Phys.* **1943**, 11, 45.
[9] Stockmayer, W.H. *J. Chem. Phys.* **1944**, 12, 125.
[10] Zhu, S. and Hamielec, A.E. *Macromolecules* **1992**, 25, 5457-5464.
[11] Gordon, M. *Proc. R. Soc. London Ser.* A **1962**, 268, 240.
[12] Macosko, C.W. and Miller, D.R. Macromolecules 1976, 9(2), 199-206.
[13] Miller, D.R. and Macosko, C.W. *Macromolecules* **1976**, 9(2), 206-211.
[14] Bowman, C.N. and Peppas, N.A. *Chemical Engineering Science* **1992**, 47(6), 1411-1419.
[15] Tobita, H. *Macromolecules* **1993**, 26, 5427-5435.
[16] Tobita, H. *Macromolecules* **1993**, 26, 836-841.
[17] Tobita, H. and Hamielec A.E. *Macromolecules* **1989**, 22, 3098-3105.
[18] Scranton, A.B. and Peppas, N.A. *J. Polymer Science: Part A: Polymer Chemistry* **1990**, 28, 39-57.
[19] Dotson, N.A. *Macromolecules* **1992**, 25, 308-321.
[20] Williams, R.J.J. *Macromolecules* **1988**, 21, 2568-2571.
[21] Williams, R.J.J. and Vallo, C.I. *Macromolecules* **1988**, 21, 2571-2575
[22] Dotson, N.A., Galvan, R. and Macosko, C.W. *Macromolecules* **1988**, 21, 2560-2568.
[23] Scranton, A.B., Klier, J., and Peppas, N.A. *Macromolecules* **1991**, 24, 1412-1415.
[24] Tobita, H. and Hamielec, A.E. *Makromol. Chem., Macromol. Symp.* **1988**, 20/221, 501-543.
[25] Hiemenz, P.C. *Polymer Chemistry*, (New York: Marcel Dekker, **1984**.)
[26] Flory, P.J. *Principles of Polymer Chemistry*, (Ithaca, NY: Cornell University Press, **1953**.)
[27] North, A.M. *The Kinetics of Free Radical Polymerization*, (New York: Pergamon Press, **1966**.)
[28] Broer, D.J., Moll, G.N. and Challa, G. *Polymer* **1991**, 32(4), 690-695.
[29] Levinos, N.J. and Harris, A.L. *AT&T Laboratories Technical Memorandum* **1992**, AT&T BL Document No. 11541-921124-66TM.
[30] Bair, H., private communication.
[31] Hale, A. and Bair, H.E. *Macromolecules* **1991**, 24, 2610-2621.

[32] McKenna T.F. and Hamielec A. E. *Polymer Handbook, 3rd Ed.*, J. Brandrup and E.H. Immergut, editors (New York, Wiley, **1989**.)
[33] Bellobono, I.R., Oliva, C. Morelli, R., Selli, E. and Ponti, A. *J. Chem. Soc. Faraday Trans.* **1990**, 86(19), 3273-3277.
[34] Doornkamp, A.T., Alberda van Ekenstein, G.O.R., and Tan, Y.Y. *Polymer* **1992**, 33(13) 2863-2867.
[35] Cook, W.D. *J. Polymer Science: Part A: Polymer Chemistry* **1993**, 31, 1053-1067.
[36] Data sheet provided by CIBA-GEIGY.
[37] Ferrara, J.A. *AT&T Laboratories Technical Memorandum* **1988**, AT&T BL Document No. 11516-881208-42TM.

5836-28